AN ANALYSIS OF HEAD IMPACT ANGLE ON THE DYNAMIC RESPONSE OF A HYBRID III HEADFORM AND BRAIN TISSUE DEFORMATION

By

Anna Oeur

A thesis submitted to the Faculty of Graduate and Postdoctoral Studies

In partial fulfillment of the requirements for the degree of

Master of Science in Human Kinetics

Advisor

Thomas Blaine Hoshizaki, PhD

Committee Members

Heidi Sveistrup, PhD

Yves Lajoie, PhD

Faculty of Health Sciences

School of Human Kinetics

University of Ottawa

December 2012

Acknowledgements

I would like to thank all the individuals who have helped me in the completion of this work. I would like to thank my family, especially mom and dad who have been so understanding and encouraging during this process. Thanks for all the love and motivation.

A special thank you goes to Dr. Blaine Hoshizaki would supervised me throughout my masters. It was a great honour to have been able to work with an outstanding researcher and leader in the field of head impact biomechanics. I would also like to thank Dr. Heidi Sveistrup and Dr. Yves Lajoie for being on my committee and reviewing my work. Their research expertise has influenced the completeness of this thesis.

I would like to thank Geoffrey, Andrew, Phil, Evan, Marshall and Clara for all their help in making this work possible. My graduate student life thus far has truly been an enriched experience with having so many people from different backgrounds with which I can exchange ideas and opinions with.

Abstract

The objective of this research was to better understand how impact angle influences headform dynamic response and brain tissue deformation. A bare headform was impacted using a pneumatic linear impactor at 5.5 m/s. The impacts were directed on the front and side location at angles of 0, 5, 10 and 15° rightward rotations as well as -5, -10 and -15° (leftward) rotations at the side to examine the characteristics of the head and neckform on the results. Peak resultant linear and rotational accelerations from the headform as well as peak maximum principal strain (MPS) and von Mises stress (VMS) estimated from a brain finite element model were used to measure the effect of impact angle. Significant results were dependent upon the impact angle and location as well as the dependent variable used for comparison ($p<0.05$). Impact angle produced significant differences in rotational acceleration and MPS at both the front and side; however angle only had an effect on VMS and linear acceleration at the front and side locations, respectively. These findings show that the effect of impact angle is asymmetrical and is specific to the dependent variable. This study suggests that varying impact angle alone may not be as influential on headform dynamic response and brain tissue deformation and that the severity of an impact may be more of a function of how both location and angle create high risk conditions.

Table of Contents

List of Tables

List of Figures

1. Introduction

1.1 Background

A large portion of the Canadian population are affected with mild traumatic brain injury or concussion with 110 out of 100 000 people affected annually (Gordon, Dooley et al., 2006). It is thought that this rate underestimates the actual number of people affected by concussion as many cases go unreported (Gordon, Dooley et al., 2006). Sports are a major contributor to the occurrence of concussion as they create environments that are high risk for injury. It has been reported that 54% of all reported cases of concussion were sports related (Gordon, Dooley et al., 2006). In a survey with Canadian varsity athletes, 70.4% of football players and 62.7% of soccer players experienced symptoms of concussion during one year of participating in their respective sports (Delaney, Lacroix et al., 2002).

The clinical definition of concussion is defined as trauma-induced changes in mental functioning that may or may not include loss of consciousness (American Academy of Neurology, 1997). Symptoms that are commonly reported as a result of concussion are headache, memory problems, fatigue, balance problems and dizziness (Blinman, Houseknecht et al., 2009). Typically, concussive symptoms resolve themselves within 3-7 days after the initial trauma; however symptoms have been reported to have lasted for several weeks (Gessel, Fields et al., 2007) . Sustaining this type of injury becomes worrisome as the cognitive dysfunction associated with concussion could pose problems for those at work or school (McCrea, Guskiewicz et al., 2003). The long-term consequences of concussion are now starting to be identified with reports of persistent post-concussive

symptoms as well as an increased susceptibility to repeated concussions (Gerberich, Priest et al., 1983).

The seriousness of concussion has warranted research to better understand the mechanisms with which these injuries occur in order to better protect against them (Cantu, 1992). Concussion can be caused by an impact causing motion of the head and brain (Meaney and Smith, 2011). This head motion is thought to translate energy from the impact to the tissue producing in tissue injury (Groat, Windle et al., 1945). In the past, research has established a link between global head motion and the resulting injury observed (Gennarelli, Thibault et al., 1982). An artifact of this has been in quantifying the magnitudes of head motion using engineering metrics such as acceleration and establishing thresholds predictive of injury (Zhang, Yang et al., 2004a).

Concussion is difficult to identify using diagnostic imaging techniques (Bailes, 2009). In most circumstances the observation of the signs and symptoms of concussion are the only evidence of injury (Cantu, 1992). In the past, studies on the mechanism of concussion have included experiments on physical, animal and cadaveric specimens (Holbourn, 1943, Gurdjian, Lissner et al., 1954, Gennarelli, Thibault et al., 1982). More recent approaches to studying concussion involve reconstructing the impact conditions responsible for causing the injury (Newman, Beusenberg et al., 2005). Generally, this biomechanical method to studying head injury includes gathering details about the event, reconstructing the incident using computational or physical tools and analyzing the results from the simulation (O'Riordain, Thomas et al., 2003).

The research surrounding the reconstruction of concussive injuries includes studying video data of head impacts from player collisions in football and rugby (Pellman, Viano et al., 2003a, Frechede and McIntosh, 2007). To reconstruct a head impact, specific variables of the head injury event are gathered such as the impact mass of players and objects, impact velocity, location, angle and compliance (Frechede and McIntosh, 2007). Knowing how each of these variables affects the results of the reconstruction helps to better understand the conditions surrounding the head impact event.

In a study by Frechede and McIntosh (2007), the authors used the computational tool Mathematical Dynamic Models (MADYMO) to simulate sports collisions. In this research, the authors preceded their simulations with a parametric study investigating the effect of different impact variables on their reconstructions. These variables included impact angle and velocity among many others. They found that impact angle did not influence the results of the reconstruction meanwhile other variables like impact velocity did. They measured the response using biomechanical measures of concussion which include peak velocity change, peak linear and rotational accelerations. One explanation that impact angle may not be as influential in these reconstructions is that these peak kinematic variables representing the motion of the head may not be sensitive enough to measure the effect of impact angle. An impact to the head can be represented by three-dimensional linear and rotational kinematics providing a more complete description of a head impact (Gilchrist and O'Donoghue, 2000).

The shape of an acceleration-time curve from an impact has been shown to influence the magnitudes and patterns of brain tissue deformation using finite element analysis (Post, Hoshizaki et al., 2012). Brain tissue deformation takes into consideration the overall shape of the acceleration-time curve in each of the three axes of motion. Brain tissue deformation

derived from finite element analysis may be a more appropriate measure to evaluate the influence of impact angle.

1.2 Study Objective

The objective of this study was to investigate the influence of impact angle on the dynamic response of a Hybrid III headform and brain tissue deformation.

1.3 Variables

1.3.1 Independent variables

1. Impact locations
    1. Front
    2. Side
2. Impact angles
    1. 0º
    2. 5º
    3. 10º
    4. 15º
    5. - 5º at the side location only
    6. -10º at the side location only
    7. -15º at the side location only

1.3.2 Dependent Variables

1. Peak resultant linear acceleration (g)
2. Peak resultant rotational acceleration (rad/s^2)

3. Peak von Mises stress (kPa)
4. Peak maximum principal strain

1.4 Hypotheses

1.4.1 Null Hypotheses

1.4.2 Peak Resultant Linear Acceleration

1. There will be no significant differences in peak resultant linear acceleration for 0°, 5°, 10° and 15° impact angles at the front impact location.
2. There will be no significant differences in peak resultant linear acceleration for 0°, 5°, 10° and 15° impact angles at the side impact location.
3. There will be no significant differences in peak resultant linear acceleration for 0°, -5°, -10° and -15° impact angles at the side impact location.

1.4.3 Peak Resultant Rotational Acceleration

1. There will be no significant differences in peak resultant rotational acceleration for 0°, 5°, 10° and 15° impact angles at the front impact location.
2. There will be no significant differences in peak resultant rotational acceleration for 0°, 5°, 10° and 15° impact angles at the side impact location.
3. There will be no significant differences in peak resultant rotational acceleration for 0°, -5°, -10° and -15° impact angles at the side impact location.

1.4.4 Peak Von Mises Stress

4. There will be no significant differences in peak von Mises stress for 0°, 5°, 10° and 15° impact angles at the front impact location.
5. There will be no significant differences in peak von Mises stress for 0°, 5°, 10° and 15° impact angles at the side impact location.
6. There will be no significant differences in peak von Mises stress for 0°, -5°, -10° and -15° impact angles at the side impact location.

1.4.5 Peak Maximum Principal Strain

7. There will be no significant differences in peak maximum principal strain for 0°, 5°, 10° and 15° impact angles at the front impact location.
8. There will be no significant differences in peak maximum principal strain for 0°, 5°, 10° and 15° impact angles at the side impact location.
9. There will be no significant differences in peak maximum principal strain for 0°, -5°, -10° and -15° impact angles at the side impact location.

1.5 Limitations

1.5.1 Hybrid III head and Neckform

The Hybrid III head and the neckform used in this study are a limitation because they are used as human surrogates to head impacts. They may not be representative of a real life impact response because they are composed of a combination of aluminum, vinyl and rubber in an attempt to mimic the movement of the head and neck from an impact where human tissues tend to be more compliant in nature. The Hybrid III head and neckform were developed for use in car crash testing and have been only validated for frontal impacts.

1.5.2 Finite Element Model

The finite element model used in this study is also a limitation of this research because it estimates human brain tissue deformations from a head impact. In order to do this, some assumptions regarding the behaviour of brain tissue have been made. The first assumption is that the constitutive properties governing the brain tissues in the model were derived from a combination of cadaver and animal experiments and is not based on live human tissue material properties which may not provide an accurate estimation of live human brain tissue deformation. Accurately modeling the complex structures and the nonlinear behaviour of human brain tissues remains a challenging task and is subject to much debate in the engineering community (Horgan, 2005).

Another limitation of this brain finite element model is that it has been partially validated against the responses of select cadaver head impact experiments available in the literature. This is a limitation because the finite element model may not provide an accurate estimation of live human brain tissue deformation. The response of cadaver heads may not be the same as those of live human heads which would make it difficult in using this model for predicting injury. These validations involved the response of the entire head and brain acting as a unit to an impact and are not specific to particular structures or tissues such as the brainstem or cerebrum. The assumptions that are made concerning the behaviour of brain tissue are specific to this model and analyses run using this tool may not produce the same results as other finite element models available.

1.5.3 Pointed Impactor Striker

The pointed impactor striker used in this study is a limitation because it affects the number of possible impact angle conditions that could be used for treatment of the dependent variables. The striker was designed to maintain similar dimensions as previous vinyl impactor strikers available for use in head impact testing specific to the pneumatic linear impactor system. The tip of the striker was modified to be smaller so that the exact same location on the headform could be impacted at different angles.

1.6 Delimitations

1.6.1 Hybrid III headform

The 50th percentile adult male Hybrid III headform was used this study because it was available for use in laboratory. This headform is a delimitation of this research because it is specific to the average male head which may not represent the response of a female headform under the same impact conditions. A 5th percentile Hybrid III female headform has been developed by First Technology Safety Systems (Plymouth MI, USA); however this model is a smaller version of the 50th percentile adult male Hybrid III headform as these dimensions (mass 4.54 kg) were scaled for the female headform (mass 3.73 kg). The inherent differences of these two models of headforms would produce characteristic dynamic responses to impact, but the relationship between the impact parameters and the headform responses is assumed to be similar for both models. Therefore, the 50th percentile adult male Hybrid III headform was used to study the relationship between impact angle and headform dynamic response.

1.6.2 Impact Locations

This research is delimited to the front and side impact locations on the Hybrid III headform. These two impact locations were chosen because they represent two different headform geometries and neckform orientations. Other impact sites could have been chosen, but for the purpose of studying the relationship between impact angle and head impact response these two locations were chosen and as such, the results were specific to these sites.

1.6.3 Impact Angles

This research is delimited to the number of impact angles used in this study, specifically 0, 5, 10 and 15° at both impact locations and -5, -10 and -15° additional angles at the side location. The maximum variation of impact angle (15°) was limited by the pointed impactor striker cap used in this study because each condition had to maintain the requirement of impacting the same location on the headform throughout the different impact angles. Larger impact angles greater than 15° created conditions where the side of the pointed impactor striker cap made first contact with the headform.

2. Literature Review

This chapter presents the literature related to concussion and the biomechanical methods used to study the mechanisms of injury. They will be introduced under the following topics: (1) Concussion Signs and Symptoms, (2) Head Injury Mechanisms, (3) Head Injury Reconstruction, and (4) Summary.

2.1 Concussion Signs and Symptoms

The clinical definition of mild traumatic brain injury (mTBI) or concussion is defined as trauma-induced changes in mental functioning that may or may not include loss of consciousness (American Academy of Neurology, 1997). Concussion has been classified as a transient type of injury where any functional impairment is typically restored after the initial insult (Dischinger, Ryb et al., 2009). In the past, much debate has gone into a complete definition of concussion including characteristic symptoms associated with this type of injury. Previously, it was thought that a patient was not considered to have suffered a concussion unless loss of consciousness was observed (Cantu, 1992). Now there is reason to disregard the presences of loss of consciousness or even amnesia as a definitive marker for concussion as a patient can sustain a concussion without having these symptoms (Cantu, 1992, McCrory, Meeuwisse et al., 2009).

Symptoms such as headache, dizziness, nausea or vomiting are usually observed within minutes to hours, meanwhile poor attention, concentration and memory have been reported within days to weeks after sustaining a concussion (Kelly and Rosenberg, 1997). Typically, most concussive symptoms resolve themselves in 3-7 days however symptoms

have been reported to last longer than 14 days in a study done on high school football players (McClincy, Lovell et al., 2006). Researchers found a similar trend with patients reporting a decrease in symptomology over a 1 year follow-up period however; some patients did report that they were still experiencing symptoms at 1 year follow up (Alves, Macciocchi et al., 1993). Other studies have suggested that the chances of experiencing a subsequent concussion are increased by up to 3 to 4 times than those who had never sustained a concussion (Gerberich, Priest et al., 1983, Delaney, Lacroix et al., 2002).

Sustaining this type of injury becomes worrisome, especially for the student athlete as data regarding the cognitive effects of concussion suggest a decrease in information processing and memory deficits that may pose problems in the workplace or school (McCrea, Guskiewicz et al., 2003). Other research has suggested motor functioning deficits are associated with concussion. The researchers, van Donkelaar, Langan et al. (2005) compared university students with sports related mTBI to a control group using an Attentional Network Test (ANT) by measuring reaction time. They found increased reaction times in students with concussion due to decreased attentional processing (van Donkelaar, Langan et al., 2005). These cumulative deficits could lead to poor outcomes in terms of school and sports for the student athlete.

An extreme outcome as a result of early return-to-play after sustaining a concussion was documented in a case study on a high school football athlete. The athlete had sustained a concussion and waited one week before returning to play. After coming back, he received a second head impact causing serious debilitation and eventually death (Kelly, Nichols et al., 1991). After the second head impact, a CT scan showed diffuse swelling throughout causing compression on various parts of his brain (Kelly, Nichols et al., 1991). An autopsy

revealed no skull fractures; however there were small brain bleeds throughout his brain as well as evidence of major swelling. This fatal consequence prompted and supported the need for return-to-play guidelines for use by physicians and athletic therapists in order to avoid future tragedies (Khan, 2009).

As a result of the seriousness of concussive injuries, research has been undertaken to better understand the mechanisms by which concussions occur. The next section focuses on research investigating head injury mechanisms.

2.2 Head injury Mechanisms

In the past, methods of studying head injury have used a combination of animal, cadaver and physical models. For the purpose of studying concussion, animal models of head injury have been used extensively in experimental research for studying the physiological, morphological and time course of concussive symptoms (Gennarelli, 1994). Experiments on cadavers as well as inanimate physical models lack the physiological response as well as the observed symptomology characteristic of concussive injuries.

2.2.1 Animal Models of Head Injury

Many different animal models of head injury have been proposed in the past: fluid percussion models, rigid percussion models, injection models, local tensile models, inertial and impact acceleration models (Gennarelli, 1994). Fluid percussion models use a small injection of fluid into the subdural space of the animal to elicit concussive symptoms and are typically characterized by a brief period of behavioural unresponsiveness. In rigid

percussion models, a small solid indenter is used to impact the dura of the animal brain; injection models use injections of blood or fluids for the purpose of studying various hematomas in the head. Local tensile models apply a suction injury to the dura of the animal to produce a cerebral contusion at the site, inertial injury models apply acceleration to the head without initial impact and impact acceleration models as the name suggests accelerates the head and brain through by impacting the head (Gennarelli, 1994).

The scope of this study is to better understand the impact conditions associated with concussive injuries, therefore of the 6 models listed, the impact acceleration model of head injury will be further explored. Although the other models of head injury are probable in producing concussive symptoms, it is more likely that concussive brain injury in humans are a result of acceleration loading to the head as opposed to direct trauma to the open dura.

2.2.2 Head Impacts

Human head injury can be the result of motion of the head and brain to some external force producing the injury (Meaney and Smith, 2011). As mentioned previously, acceleration models of head injury can be caused by two mechanisms: impact and inertial. An impact to the head produces contact forces that are applied directly to the head and can be brought on by the head impacting a slower moving or stationary object such as a fall to the ground or by the stationary or slow moving head being impacted by a faster moving object, such as a head collision in sports (Zhang, Yang et al., 2001a). Direct contact with an object causes local skull deformation at the site of impact, while increased skull deformation past a threshold will cause failure producing skull fracture (Yoganandan and Pintar, 2004). Skull fractures can lead to subsequent injuries such as brain bleeds when the fracture line

occurs over major cerebral blood vessels (Yoganandan and Pintar, 2004, Meaney and Smith, 2011). The extent of skull deformation as a result of a physical impact has been associated with pressure gradients that have been thought to be responsible for intracranial damage (Gurdjian, Webster et al., 1955).

2.2.3 Linear Acceleration

It has been hypothesized that a direct impact to the head can produce pressure waves that traverse the brain and create pressure gradients within the intracranial contents with areas of positive pressure directly underneath the impact site, coup pressures, and negative pressures are found directly opposite the impact site, countercoup pressures (Gross, 1958, Hardy, Mason et al., 2007). This hypothesis was proposed to explain the occurrence of head and brain injury that were contralateral to the impact site. This early research investigating the intracranial response to head impacts established a relationship between the internal pressure response of the brain and the external linear acceleration of the head (Gurdjian, Hodgson et al., 1968). As such, linear acceleration has been a common measure for head injury where peak resultant linear acceleration is commonly used in helmet testing standards for pass/fail criteria (Canadian Standards Association, 2009, Snell Memorial Foundation, 2010)

2.2.4 Rotational Acceleration

Indirect loading is the second mechanism of injury, which is associated with more rotational dominant types of loading applied to the head (Gurdjian, 1972). Fijalkowski, Stemper et al. (2007) studied the concussive effects of coronal plane inertial loading on

rodents (without contact). This type of loading produced mainly rotation of the head about the neck. They reported no signs of skull fractures; however the rodents were considered unconscious as signs of motor reflexes were diminished. Upon pathological examination, some rodents suffered from brain bleeds as blood was found over the cerebral hemispheres meanwhile others suffered brain swelling (Fijalkowski, Stemper et al., 2007).

Holbourn (1943) suggested that concussive type injuries could be the result of the shear and tensile strains experienced from rotational acceleration. His hypothesis was based on an experimental physical model composed of a gel-filled container subjected to pure rotation where shear and tensile strain tracts were observed (Holbourn, 1943). The observations of stretching and shearing tracts in the gel model were thought to be analogous to axonal damage under similar loading. Research by Gennarelli, Ommaya et al. (1971) also found that rotational acceleration contributed more to concussive injuries, diffuse axonal injuries and subdural hematomas than linear acceleration alone. As a result, the shear deformations caused by rotational accelerations have been proposed to be an important contributor to the mechanism of injury for concussion (Zhang, Yang et al., 2001a).

In real-life situations, an impact to the head rarely produces purely linear or purely rotational acceleration. It is more likely that combination of both types of acceleration is the result of a head impact (Meaney and Smith, 2011). In the past, researchers have made links between head acceleration and brain injury; however head acceleration may not provide enough information about the magnitude of loading responsible for injury on the neural tissues (Meaney and Smith, 2011). This has lead researchers to investigate the relationship between brain tissue stress and strain with injury (Zhang, Yang et al., 2001a). A number of different engineering metrics for materials have been proposed for measuring brain injury;

however the two variables that are used in this research to measure brain tissue deformation are maximum principal strain and von Mises stress.

2.2.5 Maximum Principal Strain

Maximum principal strain is a measure that is common in both anatomical testing of animal axons and in finite element analyses of biological materials (Gailbraith, Thibault, & Matteson, 1993; Shreiber, Bain & Meaney, 1997). As the name suggests, maximum principal strain is the greatest magnitude of strain along the principal axis of a material. That is, the greatest strain in either in the x, y or z axis will be recorded. Maximum principal strain is calculated using the following equation where ε is the strain in a given axis:

$$\varepsilon 1,2 = \frac{\varepsilon_x + \varepsilon_y + \varepsilon_z}{3} \pm \frac{\sqrt{2}}{3}\sqrt{(\varepsilon_x - \varepsilon_y)^2 + (\varepsilon_y - \varepsilon_z)^2 + (\varepsilon_z - \varepsilon_x)^2}$$

2.2.6 Von Mises Stress

Von Mises stress is a measure that is commonly used in engineering that represents a threshold variable or yielding criteria for ductile materials. Von Mises stress is the three-dimensional deformation of a material. The calculation of this variable incorporates loading in three axes (x, y and z) and is calculated using the following equation:

$$\sigma = \sqrt{0.5\left[(\sigma_x - \sigma_y)^2 + (\sigma_y - \sigma_z)^2 + (\sigma_z - \sigma_x)^2\right]} + \sqrt{+3\left(\tau_{xy}^2 + \tau_{yz}^2 + \tau_{zx}^2\right)}$$

Where σ is the normal stress in a given axis and τ is the shear stress in a given axis and is measured in Pascals (Pa). These two variables have been used in previous research of head

injury reconstructions to quantify the amount of brain tissue deformation from head impacts (Willinger and Baumgartner, 2003, Zhang, Yang et al., 2004a, Kleiven, 2007).

2.2.7 Alternative Mechanisms of Brain Injury

Another aspect to studying concussion has been to look at the neurophysiology of the brain after injury. Biochemical pathways are now being extensively studied in order to detect minute changes in the brain that could help to explain the diversity of signs and symptoms of concussion (Shaw, 2002, Smith, Uryu et al., 2003). This type of research may help to explain some of the long-term effects of concussion as well as the pathology of these types of injuries.

One of the major problems with concussive types of injuries is that neuroimaging techniques such as CT or magnetic resonance imaging (MRI) scans fail to show any structural abnormalities (Bailes, 2009). However, the long-term detrimental effects associated with sustaining repetitive concussions are starting to be documented. A disease referred to as chronic traumatic encephalopathy (CTE) has been associated with a history of repeat concussions as the condition was found in an autopsy of a football player in the National Football League (NFL) (Omalu, DeKosky et al., 2005). The subject was diagnosed with severe major depressive disorder and committed suicide 12 years after retirement from the league. A major finding during the autopsy revealed protein deposits that were present in all regions of the brain (Omalu, DeKosky et al., 2005). This accumulation of protein plaques in the brain has been put forth as a mechanism of head injury resulting from biochemical cascades of the cells as a result of head trauma (Smith, Uryu et al., 2003).

A new experimental neuroimaging technique for studying patients with concussion symptoms has been suggested by Niogi, Mukherjee et al. (2008). Patients with mild traumatic brain injuries (mTBI) underwent diffusion tensor imaging (DTI) to assess microstructural changes associated with post-concussive symptoms. Diffusion tensor imaging is an imaging tool that measures the integrity of the white matter tracts using the diffusion patterns and rates of water molecules in the axons, where damaged tissues have less ordered water diffusion (Le Bihan, Mangin et al., 2001). To be included in the study, subjects were required to have a least one persistent symptom from a pre-determined checklist of symptoms including, headaches, fatigue, dizziness, irritability, personality changes, or apathy. Their imaging techniques revealed that white matter fibers of the frontal and temporal lobe as well as fibers of the corpus callosum were damaged (Niogi, Mukherjee et al., 2008). A limitation of DTI is that it would not be able to detect cellular structural changes in other types of tissues other than white matter.

2.3 Head Injury Reconstruction

Due to the elusive nature of concussive injuries, traditional methods for studying head injury make it difficult as macroscopic abnormalities are not always apparent with patients sustaining a concussion and the outcomes associated with it vary from one patient to the next. More recent methods to studying the biomechanics of concussion have used reconstruction of the events causing the injury. This method has allowed researchers to make links between engineering parameters with signs and symptoms of concussion in an attempt to quantify the injury and its severity.

Research on concussions has used reconstructions of player collisions in sporting events. Elite contact sports such as football and rugby have allowed researchers to obtain video recordings of the matches and subsequently player collisions that have caused (Pellman, Viano et al., 2003b, Frechede and McIntosh, 2007). The process of reconstruction typically involves an analysis of the incident to obtain details of the impact conditions producing injury. Secondly, the incident is simulated using a variety of tools such as a physical reconstruction with anthropometric dummies, computational and numerical simulations involving finite element analysis or Mathematical Dynamic Models (MADYMO). This process provides researchers with a method for quantifying the injury based on commonly used engineering metrics. This approach can help to establish levels with which concussive injury occurs and help researchers develop methods to reduce or eliminate conditions that would produce injury.

Football player collisions obtained from the National Football League (NFL) has been widely used as a database for reconstruction. Cases of player collisions resulting in concussion and those without were physically reconstructed using anthropometric dummies (Pellman, Viano et al., 2003b). Careful video analysis of the events were undertaken to obtain details of the variables crucial for the reconstruction. From the video analysis, relative speed, impact location and angle of the player's heads were estimated (Newman, Beusenberg et al., 1999). These variables served as input parameters characterizing the impact conditions with which two Hybrid III head, neck and torso dummies were collided. The dummies were equipped with accelerometers to measure the associated linear and rotational accelerations from the helmeted head impacts (Newman, Beusenberg et al., 1999).

A separate study by Viano, Casson et al. (2005) took these head kinematic data from the NFL reconstructions and used them as input into a finite element model of the brain. The Wayne State University Brain Injury Model (WSUBIM) was used to run computer simulations of the brain to these helmeted impacts. These results illustrated that strain concentrations migrated throughout the brain during these helmeted impacts (Viano, Casson et al., 2005).

2.3.1 Finite Element Analysis

Past research tools and methods to studying head injury have used human head surrogates to approximate the response of the head and brain to impact. These surrogates include using animal, physical models as well as cadavers for experimentation as ethical issues arise with undertaking human head impact research. Each of these surrogates used in head injury research have both advantages and disadvantages. Animal experimentation allows for the physiological manifestations of a concussive injury to be studied, however problems arise in the applicability of these results to humans (Gennarelli, 1994). Experimental studies conducted on cadavers have the added benefit of having the same geometry and mass distributions as living humans; however the disadvantages of using these types of specimens include the unknown effects of tissue desiccation from embalming as well as a lack of a physiological response to head impact (Gilchrist and O'Donoghue, 2000, Yoganandan, Pintar et al., 2009). Anthropometric testing devices (ATDs) are widely used in motor vehicle crash testing, but these devices are limited in their ability to directly measure microscopic strain responsible for brain injury; however they are advantageous because they

allow crash impact testing to be undertaken in a consistent and reliable manner (Dimasi, Eppinger et al., 1995).

Advances in computer technology have allowed researchers to create sophisticated computer models of the brain to predict the intracranial response to head motion (Horgan and Gilchrist, 2003). Finite element models allow estimates of soft tissue strains caused by linear and rotational accelerations from dynamic impacts that may be associated with injury(Dimasi, Eppinger et al., 1995). Since brain deformation has been linked to brain injury, finite element analysis may be a more appropriate tool for studying the risk of concussion (King, Yang et al., 2003).

Finite element analysis is an engineering tool that approximates the response of a physical system to loading. Finite element analysis in this research would aid in studying the response of the human head and brain to impact. To obtain the most accurate approximation of how the head and brain are to respond to impact in real life, the finite element model should have accurate constitutive properties that represent the various tissues types as well as geometries associated with the different brain structures. The finite element model of the brain is comprised of a number of formulations that incorporate the mechanical properties along with constants governing how each material is to respond to loading. Like most biological materials, the brain exhibits a non-linear response to loading that is dependent upon the rate and duration of the applied loads. The time dependency of biological material is a characteristic of the viscoelastic response of the material (Horgan, 2005). As such, the following shear modulus equation (G(t)) was used in the model to represent the viscoelastic behavior of the tissue:

$$G(t) = G_\infty + (G_0 - G_\infty)e^{-\beta t}$$

The long-term shear modulus is represented by G_∞, the short-term modulus, G_0 and β represents the decay factor (Horgan and Gilchrist, 2004). A unique G_∞, and G_0 constant for each tissue represents the time dependent response of that particular tissue to shear loading. This algorithm incorporates loading of the different tissues in the results of the simulation.

A second group of researchers undertook concussion reconstruction; however instead of using physical reconstruction with anthropometric dummies coupled with finite element analysis, MADYMO was used to simulate the injury. MADYMO is a rigid body computational model that was used to simulate real-life concussive impacts obtained from rugby and Australian football matches (Frechede and McIntosh, 2007). In an attempt to better understand the reconstruction process and how variables used to describe the impact conditions influence the overall simulation, the authors performed a series of parametric tests. In these tests, variables such as impact velocity, location, angle, neck stiffness as well as other MADYMO parameters were varied during the simulation. Peak linear and rotational accelerations and peak change in velocity as well as other kinematic measures were used to determine the influence of each of the variables on the simulations (Frechede and McIntosh, 2007). Of these variables, impact location, velocity and parameters describing the model were found to be influential in the results of the simulation when evaluated using these measures, meanwhile neck stiffness and impact angle variations of 20° had little to no influence (Frechede and McIntosh, 2007). Understanding how these impact variables influence the reconstruction are important when trying to choose suitable and accurate impact conditions.

In accordance with these findings, impact location has been shown to be influential in brain tissue deformation magnitudes. Experimental research by Zhang, Yang et al. (2001c) conducted a study investigating the directional sensitivity of the head using finite element analysis to frontal and lateral impacts of the same impact energy. They found that lateral impacts produced higher magnitudes of skull deformation, intracranial pressures and tissue stress and strain (Zhang, Yang et al., 2001c). Kleiven (2003) used a finite element model of the brain to investigate the influence of loading direction on the brain and bridging veins in the prediction of subdural hematoma. Rotational impulses produced larger relative motion between the skull and brain as well as higher strain in the bridging veins than translational impulses. The author concluded that impact direction varies the tissue response of the skull and brain (Kleiven, 2003).

Impact location has also been shown to be important to consider with various animal studies. Gennarelli, Thibault et al. (1982) conducted research on directional dependent loading on primates and measured the onset of concussion and the duration of loss of consciousness. From this research, it was concluded that the duration, degree and outcome of neuropathological abnormalities were dependent upon the direction of loading, where lateral loading produced the worst outcomes followed by oblique loading followed by sagittal loading (Gennarelli, Thibault et al., 1982, Gennarelli, Thibault et al., 1987). Hodgson, Thomas et al. (1983) conducted experiments on anesthetized monkeys and found that impacts to the tempo-parietal region were more likely to produce cerebral concussion than frontal, occipital and crown impacts. These studies demonstrate the directional sensitivity of the brain to loading, however were limited in the applicability to human brain injury. The brain mass and size of these animals is not the same as the human brain and

would undergo different patterns of tissue deformation (Ueno, Melvin et al., 1995). These studies confirm the importance of choosing representative impact locations for reconstructive purposes, as differences in brain responses leading to injury are dependent on the impact location.

2.3.2 Finite Element Model Validation

Validation of the model involved comparisons with data from cadaver head impact experiments. Intracranial pressure validations were done using Nahum, Smith et al. (1977) and Trosseille, Tarriere et al. (1992) cadaver experiments. Nahum, Smith et al. (1977) cadaver head drop test had pressure transducers located at particular regions in the head to measure the pressure associated with the head drops. To replicate these loads, a 7000 N force was applied to the frontal area of the head for a 6 ms duration and pressure-time histories were recorded in the simulation. In Trosseille, Tarriere et al. (1992) experiment, a 23.4 kg impactor travelled at 7 m/s to the facial region of a seated cadaver. A 12 accelerometer array was used to measure three axes of linear and rotational acceleration along with implanted pressure transducers to measure the intracranial response associated with impact. For validation with the UCDBTM, the linear and rotational accelerations inputs were applied to the centre of gravity of the model and the pressure-time histories were compared with Trosseille et al.'s data (1992).

Relative brain-skull displacement validation was completed by comparing Hardy, Foster et al. (2001) cadaver experiments to the model simulations. In this study, brain motion was tracked using neutral density targets that could be identified using x-ray imaging (Hardy, Foster et al., 2001). These targets were implanted into the brain tissue of cadavers

where relative brain-skull displacement was recorded after a head impact. The results of the simulations were in good agreement with the head impact responses of the cadaver experiments (Horgan and Gilchrist, 2004).

The three-dimensional linear and rotational acceleration-time curves from the impacts were used as input into a finite element model of the brain. This type of analysis allowed for the calculation of the resulting brain tissue response from the headform accelerations.

2.4 Research Problem

As impact location on the head is an important variable to consider when undertaking the reconstruction method, the importance of impact angle has been less studied and understood. As mentioned previously, Walsh, Rousseau et al. (2011) investigated the response of a Hybrid III headform to different impact conditions that included various impact locations on the head involving 45° angles. It was found that certain impact conditions that incorporated the 45° angle produced higher peak rotational acceleration than peak linear acceleration when compared to the conditions that had the same impact location but with no change in angle. These researchers concluded that certain impact conditions (combinations of location and angle) produce higher accelerations of the head than others conditions which may contribute to the risk of injury (Walsh, Rousseau et al., 2011). In this study, the authors' objective was to determine impact conditions that would elicit different relative magnitudes of acceleration by creating conditions that varied both impact location and angle. The impact conditions in this study were oriented in a manner that lined up the impactor striker at a specific site on the headform for the impact location and a headform

rotation of 45° constituted a change in impact angle. Although impact angle was varied in this study to produce different impact conditions, it was not an objective of the study to examine the effect of angle.

Upon closer examination of this study by Walsh, Rousseau et al. (2011) in light of impact angle, the impactor striker used made it difficult to isolate the effect of this variable on the results. The large diameter of this particular striker caused interactions between with the headform where different headform sites ended up being impacted for the conditions that included an angle variation (Figure 1). Therefore, understanding the influence of impact angle on headform dynamic response has yet to be fully understood.

In theory, a change in the angle of the applied vector to the head would produce a different kinematic response when represented with three-dimensional linear and rotational acceleration components (Gilchrist and O'Donoghue, 2000). It is possible that using peak acceleration measures when studying the effect of angle does not provide enough information to measure the subtleties of this variable as mentioned previously (Frechede and McIntosh, 2007).

Post, Hoshizaki et al. (2012) investigated the shape of the acceleration-time curves and their influence on brain tissue deformation metrics using finite element analysis. The peak accelerations were maintained at the same magnitude but the shapes of the acceleration-time curves were different. From this research it was concluded that the magnitude and distribution of brain tissue deformation is dependent upon the shape of the acceleration-time curve (Post, Hoshizaki et al., 2012). As such, previous studies attempting to understand the influence of impact angle may not have accurately evaluated this variable

with using only kinematic response variables such as linear and rotational acceleration. It may be more appropriate to evaluate the effect of impact angle using brain tissue deformation metrics, as an impact to the head at different angles would produce characteristic three-dimensional acceleration-time curves. A finite element analysis of these results would incorporate the shape of these curves when estimating brain tissue deformations and may provide a more appropriate means to evaluate the effect of impact angle. Furthermore, a brain tissue analysis would provide a better understanding of impact angle and may help to shed light on considering the importance of this variable in the context to head injury reconstructions.

Figure 1: Large modular elastommer programmer pad (MEP) striker

2.5 Summary

Concussion is a major health concern as a large portion of the population is affected by this injury. Past research involving animal, cadaveric and physical experiments have provided valuable information regarding the mechanisms of head injury. Due to the elusive nature of concussive injury and the diverse signs and symptoms reported, studying the

mechanism of concussion in humans remains a challenging task. Head injury reconstruction serves as a means by which researchers can investigate the mechanism of concussion. Reconstruction techniques include physical, mathematical and computational tools to re-enact the head injury event. Many different variables are important to consider when attempting to accurately simulate a head injury event. The importance of impact angle in a head injury reconstruction has not been adequately studied in the past, as peak kinematic variables may not have adequately described the effect of impact angle. A finite element analysis using brain tissue deformation metrics may be a more appropriate measure when evaluating the influence of impact angle on the head.

3. Methodology

To study the influence of impact angle on headform dynamic response and brain tissue deformation, this methodology incorporated physical impacts directed at a Hybrid III headform in a combination with finite element analysis of the brain. The headform dynamic responses from the impacts were used as input into a finite element model of the brain where brain tissue deformation was estimated.

3.1 Equipment

3.1.1 Pneumatic Linear Impactor

A pneumatic linear impactor was used to impact a bare headform. The linear impactor system is composed of a steel frame that supports an impacting arm, a piston and a pressurized air tank (Figure 2). The piston uses pressurized air from the air tank to propel the impacting arm forward at a set velocity. The pressurized air-tank is consistent in maintaining the velocity of the arm to ± 2% of the specified velocity which is in accordance with helmet testing standard for ice hockey (Canadian Standards Association, 2009)This impactor arm is directed at a sliding table situated at the end of the system. The impacting arm weights 13.1 ± 0.01 kg and was covered by a pointed nylon impactor striker cap.

Figure 2: Pneumatic linear impactor with pointed impactor striker

3.1.2 Pointed Impactor Striker

The pointed impactor striker is composed of a nylon base piece that is 90.0 mm in diameter and 25.0 mm in height (Figure 3). The base is covered by a 25.0 mm thick 60 shore A modular elastommer programmer (MEP) pad with 45º sides directing towards the centre and is covered with a nylon cap. A smaller striker cap with a decreased impacting surface area was required in order for each of the impact conditions to be adequately studied.

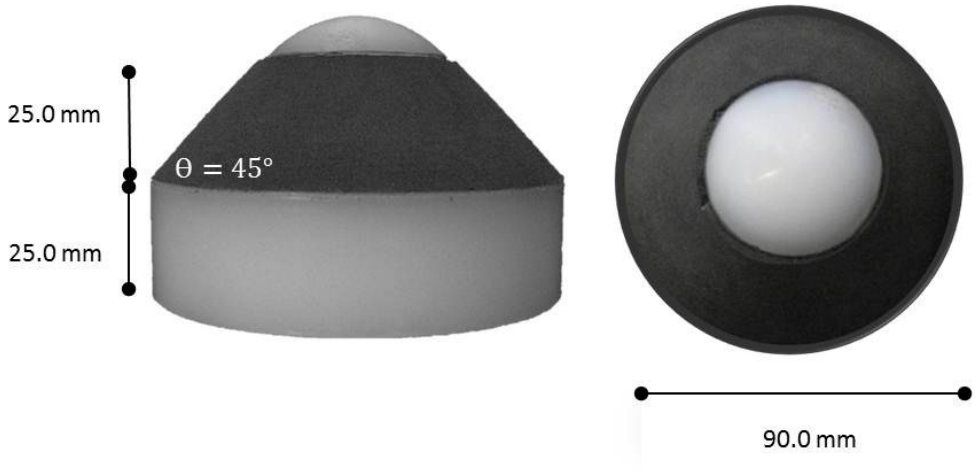

Figure 3: Pointed MEP Nylon Striker

A pilot study was conducted comparing impact angles of 0° (impact vector applied perpendicular to the headform) and 30° (headform rotated 30° rightwards) at the side location of the Hybrid III headform (refer to B in Figure 4) . The image on the right illustrates the adjusted set-up to ensure that first contact was made at the side location on the headform. As a result, the edge of the impactor striker impacted the headform. Thereby, hitting the same location of the headform at different angles was not possible using the center of this larger striker. This study was completed using a larger striker (124 mm in diameter) commonly used in head impact research (Pellman, Viano et al., 2006, Rousseau and Hoshizaki, 2009, Walsh, Rousseau et al., 2011).

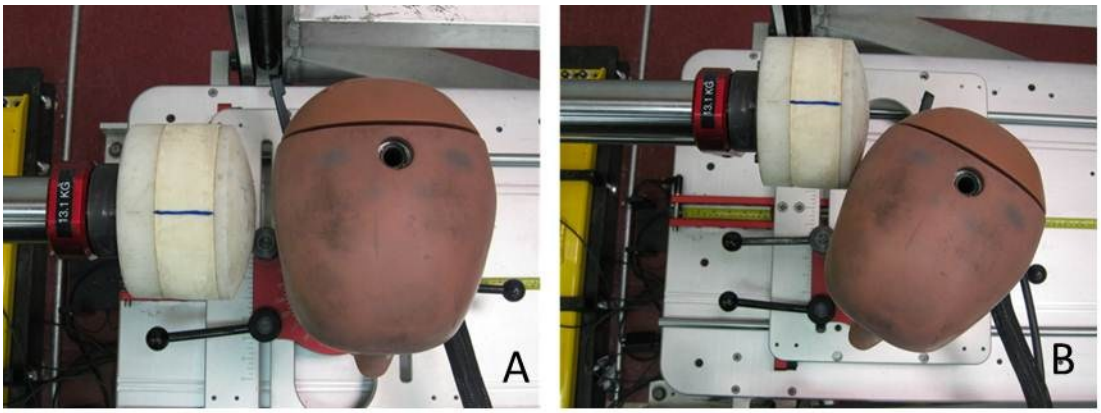

Figure 4: Illustration of the interaction between the Hybrid III headform and the large impactor striker used in the pilot study

This striker was originally developed to mimic the curvature of a typical American football helmet (Figure 1). The center of this striker cap was unable to make first contact with the headform when angle was varied due to the geometry of the headform as well as the curvature of the striker cap. Therefore, a pointed striker was use in place of the large striker to study the effect of angle (Figure 5).

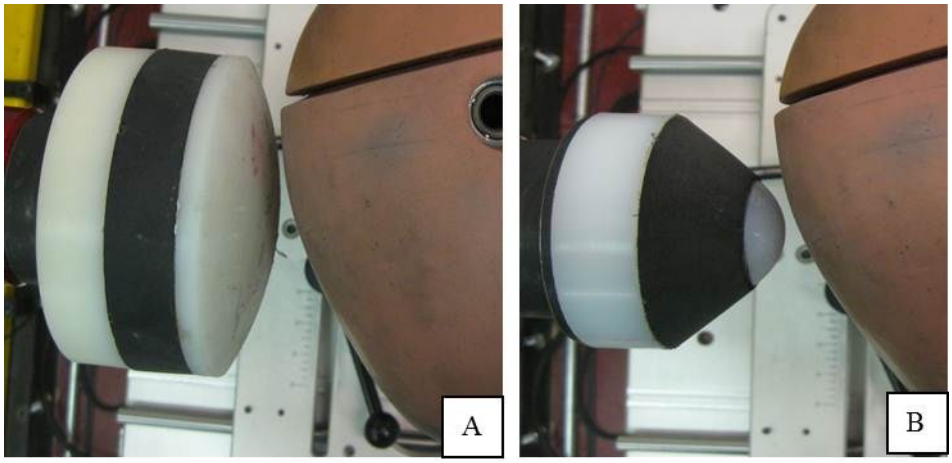

Figure 5: A comparison of the large impactor striker (A) and the pointed impactor striker (B) set-up for a -15° condition at the side

3.1.3 Sliding Table

The sliding table ran on ball bearings installed on the bottom of the table that allowed it to slide backwards with little resistance upon impact (**Error! Reference source not found.**). The table was able to translate backwards 0.54m after impact. This system was built to simulate a collision-type of impact. A foam braking system was used to stop the headform and sliding table after impact. The mass of the table is 12.782 ± 0.001 kg. A movable locking base on the table served to attach the headform. This movable locking base allowed the headform to be oriented in five degrees of freedom: fore-aft (x), lateral (y) and up-down (z) translation, as well as fore-aft (y) and axial rotation (z) and to remain fixed in position during testing. The pneumatic linear impactor, sliding table set-up and pointed impactor striker was chosen based on the ability to control impact angle and location of the headform as well as controlling for consistent impact velocities of the impacting arm in between trials.

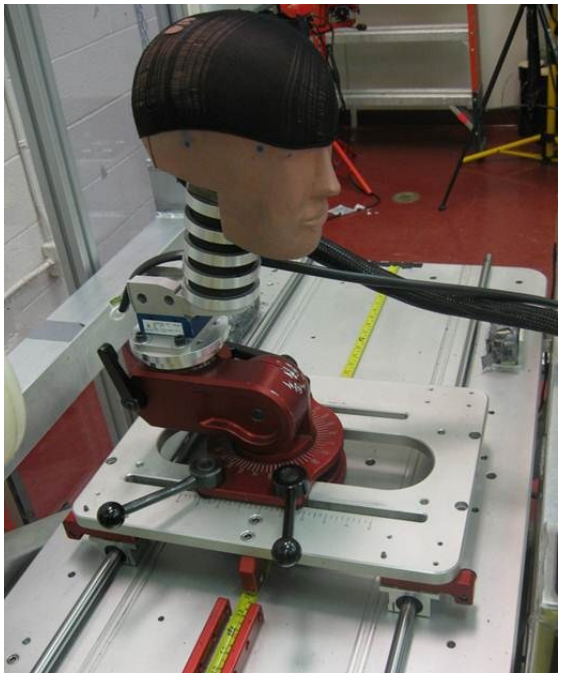

Figure 6: Sliding table with Hybrid III head and neckform attached

3.1.4 Hybrid III Head and Neckform

A 50th percentile male Hybrid III head and neckfrom (FTSS, Plymouth MI, USA) was used in this study (Figure 7). The Hybrid III neckform had a mass of 1.54 ± 0.05 kg and is composed of four butyl rubber disks that are interlocked between five aluminum plates and was developed based on cadaver data (Yoganandan, Pintar et al., 2009). The Hybrid III headform was also based on cadaveric data and was designed to respond similarly to the human head to impact (Yoganandan, Pintar et al., 2009). The headform had a mass of 4.54 ± 0.01 kg and was equipped with 9 single-axis Endevco 7264C-2KTZ-2-300 accelerometers. These accelerometers have an acceleration measurement range of 500 peak g and are calibrated by First Technology Safety System (Plymouth MI, USA). These accelerometers were positioned in an orthogonal 3-2-2-2 array as suggested by Padgaonkar, Krieger et al. (1975) in order to measure the three-dimensional kinematic response of the headform. Three

accelerometers were mounted at the center of gravity of the headform, two at the front surface (F), two on the side (S) and two on the top (T).

The following equations were used to calculate rotational accelerations based on first principles of rigid body dynamics and linear accelerations:

$$\vec{\alpha_x} = \frac{\vec{a_{zS}} - \vec{a_{zC}}}{2S} - \frac{\vec{a_{yT}} - \vec{a_{yC}}}{2T} \quad (1)$$

$$\vec{\alpha_y} = \frac{\vec{a_{xT}} - \vec{a_{xC}}}{2T} - \frac{\vec{a_{zF}} - \vec{a_{zC}}}{2F} \quad (2)$$

$$\vec{\alpha_z} = \frac{\vec{a_{yF}} - \vec{a_{yC}}}{2F} - \frac{\vec{a_{xS}} - \vec{a_{xC}}}{2S} \quad (3)$$

Where α was the x, y and z axis rotational accelerations which are derived from the x, y and z axis linear accelerations measured directly from the accelerometers. S, T, and F are the distances of the accelerometers at the side, top and front respectively from the those at the center of gravity of the headform (Padgaonkar, Krieger et al., 1975). There are other methods available for determining rotational acceleration such as the 2-D inline method and using direct rotational accelerometers for measurement.

Newman, Beusenburg, Shewchenko et al. (2005) compared these methods for measuring rotational acceleration and found that the differences in acceleration between each method were less than 6% concluding that any method would be acceptable. These authors also found that using a direct rotational accelerometer produced a noisy signal and would not be ideal for use with direct impacts to the headform. However, the 2-D inline method and the 3-2-2-2 array were suitable for these kinds of impacts, but the 3-2-2-2 method was shown to be more convenient because it used 9 accelerometers as opposed to 18

as specified by the 2-D inline method and was based on computational algorithms that are robust and accurate (Newman, Beusenberg et al., 2005).

Accelerations were collected at a frequency of 20 kHz for 20 ms of data. Data collection was initiated when the accelerations passed a 3 g threshold. The linear and rotational acceleration-time curves were recorded using TDAS Pro Lab system and software (Diversified Technical Systems, Seal Beach, California). The impact velocity was captured using an electronic time gate with National Instruments VI-Logger software (Austin Massachusetts, Texas) and were further analyzed with Bioproc 2 (developed by D.G.E Robertson, University of Ottawa). The electronic time gate was validated using a High Speed Imaging PCI-512 Fastcam, which recorded the impact at a frequency of 2 kHz using Phototron Motion Tools (San Diego, California). Video footage of the impactor arm striker was digitized prior to impact to determine the distance traveled over time with which impact velocity was calculated.

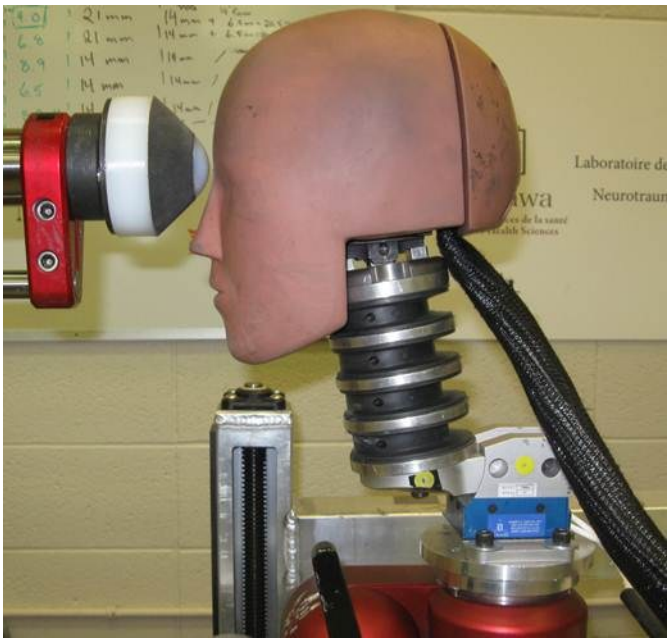

Figure 7: 50th percentile adult male Hybrid III head and neckform

3.1.5 University College Dublin Brain Trauma Model

A finite element model of the brain developed at the University College Dublin named the University College Dublin Brain Trauma Model (UCDBTM) was used in this research (Figure 8). The model of the head and brain are comprised of approximately 26 000 elements representing the scalp, skull, pia, falx, tentorium, CSF, grey and white matter, cerebellum and brain stem. The skull and brain geometry of the UCDBTM were derived from computed tomography (CT) and magnetic resonance imaging scans (MRI) of a male human cadaver (Horgan and Gilchrist, 2004). The cerebral spinal fluid (CSF) was modeled using solid elements with low shear moduli to allow for a slip layer to exist between the skull and brain (Horgan and Gilchrist, 2004).

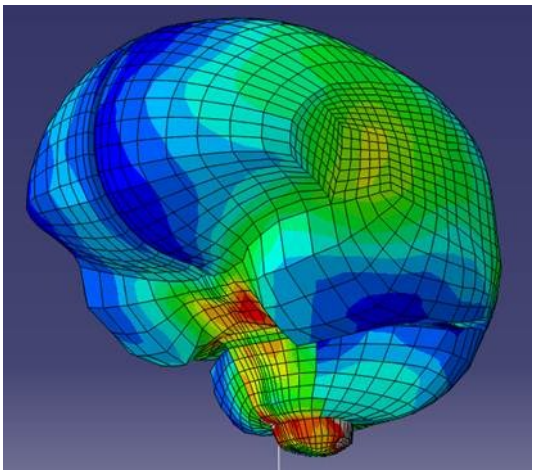

Figure 8: Image of the University College Dublin Brain Trauma Model (UCDBTM)

The characteristics constituting the different tissues in the brain were taken from the literature (Willinger, Taleb et al., 1995, Gilchrist and O'Donoghue, 2000, Zhang, Yang et al., 2001b, Horgan and Gilchrist, 2003). Table 1and 2 are lists of the different brain materials and their properties of the UCDBTM (Horgan and Gilchrist, 2003).

Table 1: UCDBTM material properties

Material	Young's Modulus (MPa)	Poisson's Ratio	Density (kg/m³)
Scalp	16.7	0.42	1000
Cortical Bone	15 000	0.22	2000
Trabecular Bone	1000	0.24	1300
Dura	31.5	0.45	1130
Pia	11.5	0.45	1130
Falx	31.5	0.45	1140
Tentorium	31.5	0.45	1140
CSF	-	0.5	1000
White Matter	Hyperelastic	0.499997	1060
Grey Matter	Hyperelastic	0.499998	1060

Table 2: Tissue characteristics for different regions of the brain in the UCDBTM

	Shear Modulus (kPa)		Decay Constant	Bulk Modulus
	G_0	G_∞	(s^{-1})	GPa
Grey Matter	10	2.0	80	2.19
White Matter	12.5	2.5	80	2.19
Brain Stem	22.5	4.5	80	2.19
Cerebellum	10	2.0	80	2.19

3.2 Procedure

A pneumatic linear impactor was used to impact a 50th percentile adult male Hybrid III head and a neckform attached to a sliding table. The headform was impacted three times per condition at a velocity of 5.5 m/s. Statistical power was determined from the pilot data by performing a post-hoc power analysis. An observed power of 99.8% was found for 3 impacts per condition. A velocity of 5.5 m/s was chosen because a peak resultant linear acceleration of 97.7 g determined from the pilot study for a side impact using the large impactor striker is associated with a high probability of concussion. Zhang, Yang and King

(2004) proposed that 66, 82 and 106 g correspond to a 25, 50 and 80% probability of sustaining a concussion.

3.3 Impact Conditions

The headform was impacted at the front and side locations at different angles. Figure 9 illustrates the impact conditions used in this study. The impact angles were a 0º angle which constitutes an impact vector directed perpendicular to the headform, 5°, 10° and 15° rightward rotation of the headform in the horizontal plane from the 0° condition. These angles were used for both the front and side impact locations; however the side locations had three additional angles of -5°, -10° and -15° leftward rotations to examine the effect of the head and neckform characteristics on the results. The positive impact angles represent a rightward rotation of the headform in the transverse plane and negative angles refer to a leftward rotation. Table 3 illustrates the research design for the study where there are a total of 11 impact conditions which were impacted 3 times each for a total of 33 impacts.

Table 3: Research design for impact location and angle

	B1	B2	B3	B4	B5	B6	B7
A1	A1B1	A1B2	A1B3	A1B4	_	_	_
A2	A2B1	A2B2	A2B3	A2B4	A2B5	A2B6	A2B7

Where:

A1 = Front

A2 = Side

B1 = 0º

B2 = 5º

B3 = 10º

B4 = 15º

B5 = -5º

B6 = - 10º

B7 = - 15º

Fifteen degrees was chosen as the maximal impact angle variation in this study because attempting to achieve a larger angle creates impacts where the side of the striker makes first contact with the headform changing the impact condition altogether. Each impact condition was set up with the guidance of a laser to ensure that the center of the striker was directed at the exact same location on the headform for all impact angles.

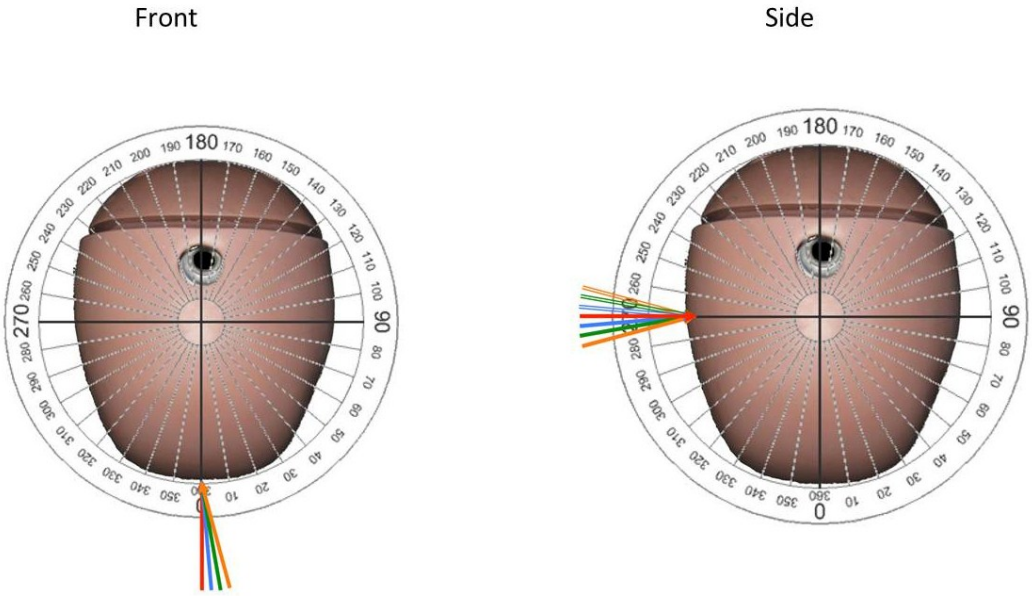

Figure 9: Front and side impact conditions where different angle conditions were obtained by rotating the neck in the transverse plane. Red represents the impact angle oriented at 0°; blue represents 5°; green represents 10° and orange represents 15°. The solid arrows represent positive impact angles and the double lined arrows represent the negative impact angles (only at side location)

3.4 Statistical Analyses

All data are expressed as a mean and standard deviation. Eight one-way ANOVAs with the independent variable of "impact angle" (4 levels: 0º, 5º, 10º, 15º rotations and 0º , -5º, -10º, -15º rotations at the side location only) were used to analyze each of the four dependent variables: peak resultant linear and rotational accelerations and peak von Mises stress and maximum principal strain for each impact location (front and side). When significance was found for impact angle, a post hoc analysis was performed using the Tukey method. The probability of making a Type I error in all tests was $P<0.05$. All analyses were performed using the statistical software package SPSS 16.0 for Windows (SPSS Inc. Chicago, IL, USA).

4. Results

The objective of this study was to investigate the influence of impact angle on headform dynamic response and brain tissue deformation. This study was comprised of 11 impact conditions which were impacted 3 times per condition for a total of 33 impacts. The impacts were carried out at 5.5 m/s at both the front and side locations at the following impact angles: 0°, 5°, 10°, 15° at both locations and -5°, -10° and -15° additional angles at the side location to see if these relationships remained the same given the features of the neckform. The mean and standard deviations for peak resultant accelerations and peak brain tissue deformations are shown in Table 4.

Table 4: Mean peak resultant linear and rotational accelerations and mean peak maximum principal strain and von Mises stress results for the front and side impact locations with 1 standard deviation in brackets

Location	Angle (°)	Peak Linear Acceleration (g)	Peak Angular Acceleration (rad/s²)	Maximum Principal Strain	Von Mises Stress (kPa)
Front	0	165.6 (0.9)	8083 (187)	0.515 (0.03)	15.89 (1.20)
	5	162.2 (3.3)	8282 (102)	0.496 (0.04)	15.23 (0.74)
	10	165.6 (5.6)	8778 (128)	0.558 (0.01)	16.62 (0.43)
	15	169.8 (1.6)	9939 (70)	0.610 (0.01)	18.77 (0.37)
Side	-15	174.5 (4.0)	11964 (346)	0.634 (0.02)	20.25 (0.65)
	-10	171.7 (2.1)	11145 (106)	0.602 (0.01)	19.54 (0.50)
	-5	164.5 (3.0)	10642 (603)	0.561 (0.02)	18.60 (0.40)
	0	164.7 (7.1)	11067 (244)	0.557 (0.02)	19.02 (1.02)
	5	162.3 (2.6)	10934 (153)	0.548 (0.01)	19.66 (0.42)
	10	161.4 (0.7)	11034 (136)	0.527 (0.01)	19.09 (0.50)
	15	159.8 (1.5)	11121 (275)	0.568 (0.01)	18.62 (0.79)

4.1 Linear Acceleration

For peak resultant linear acceleration, there was no main effect for impact angle at the front location [F (3, 8) = 2.59, p = 0.125] but there was a main effect at the side location [F (6, 14) = 7.001, p = 0.001]. Figure 10 shows the results for impact angle at the front location.

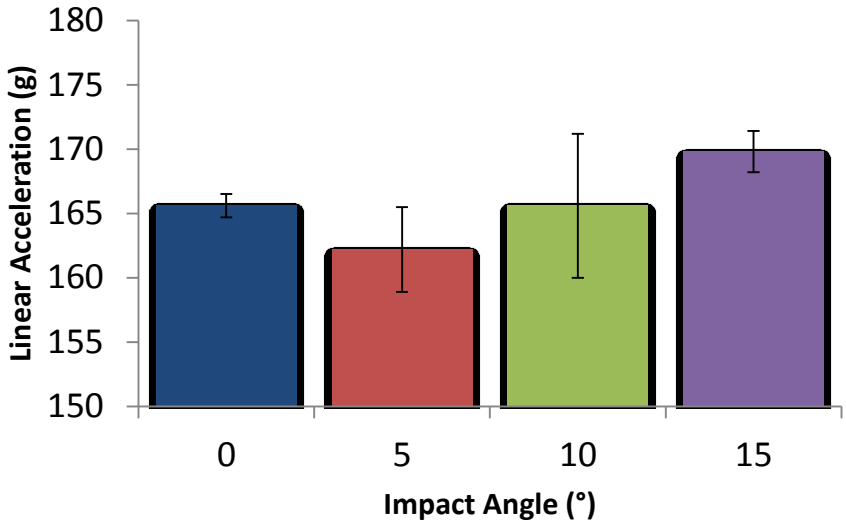

Figure 10: Peak resultant linear acceleration (g) for 0°, 5°, 10° and 15° impact angles at the front location with ± 1 standard deviation indicated in bars

At the side, no significance was found for the positive angles (Figure 11), however amongst the negative impact angles, the -15° condition produced higher values of linear acceleration than the -5° condition with 174.5 g compared to 164.5 g (p=0.05) as shown in Figure 12 with the green bracket. Also, the -15° condition produced higher levels of acceleration than the 0° condition but this relationship was not found to be significant (p=0.057).

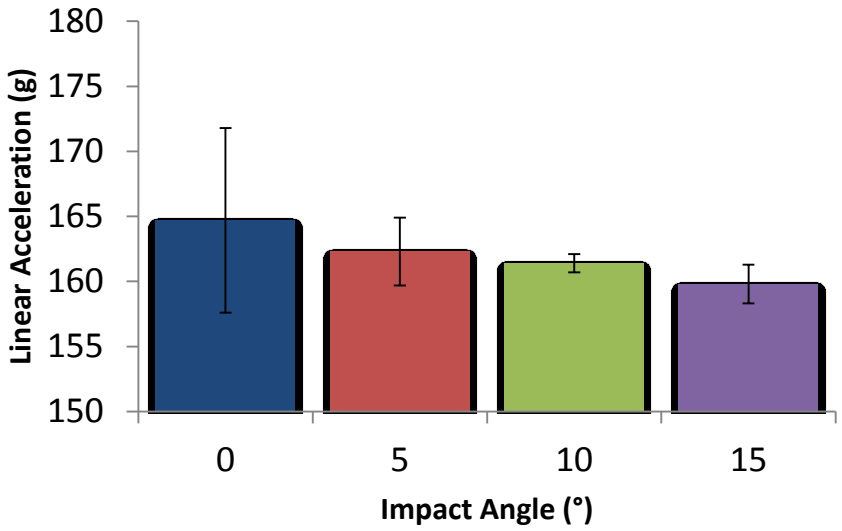

Figure 11: Peak resultant linear acceleration (g) for 0°, 5°, 10° and 15° impact angles at the side location with ± 1 standard deviation indicated in bars

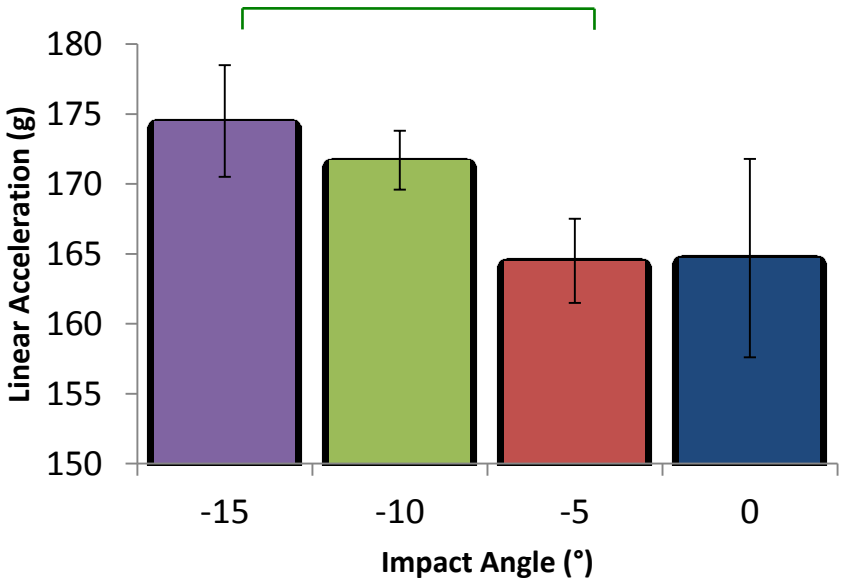

Figure 12: Peak resultant linear acceleration (g) for 0°, -5°, -10° and -15° impact angles at the side location with ± 1 standard deviation indicated in bars. A green bracket indicates a significant relationship.

4.2 Rotational Acceleration

A different relationship was found for impact angle when measured using peak resultant rotational acceleration. There was a main effect of angle at the front [$F(3, 8) = 124.50$, $p < 0.001$] where the and 15° condition had a significantly higher rotational acceleration than the 0°, 5° and 10° impact conditions ($p < 0.05$). Also, the 10° condition had significantly high rotational accelerations than the 0° and the 5° condition ($p<0.05$). The 0° and the 5° conditions were not significantly different from each other ($p=0.304$) as indicated by the red bracket in Figure 13.

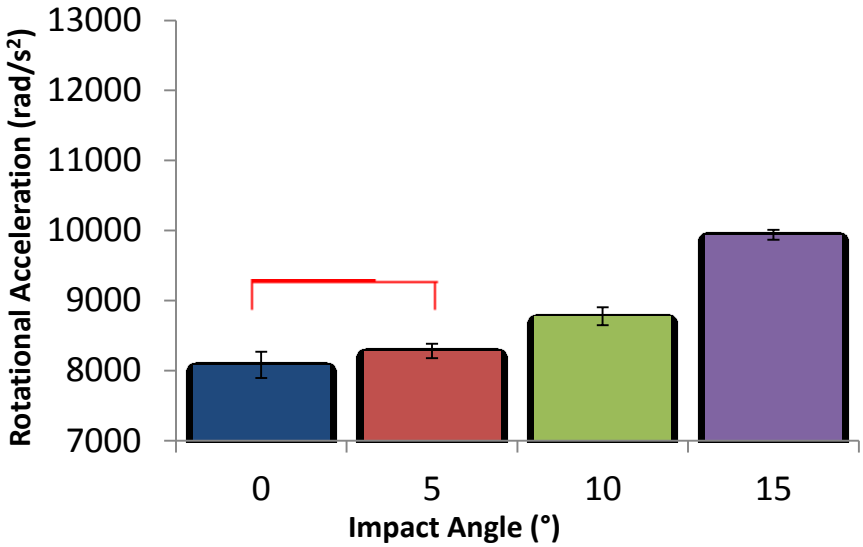

Figure 13: Peak resultant rotational accelerations (rad/s^2) for 0°, 5°, 10° and 15° impact angles at the front location with ± 1 standard deviation indicated in bars. A red bracket indicates no significant relationship between angles

There was a main effect of impact angle at the side location [$F(6, 14) = 5.14$, $p=0.006$] where no significant differences was found amongst the positive impact angles (Figure 14), however the negative impact angles produced significantly different rotational accelerations (Figure 15). The -15° condition had higher accelerations than the 0° and the -5° conditions ($p = 0.039$ and $p = 0.002$ respectively).

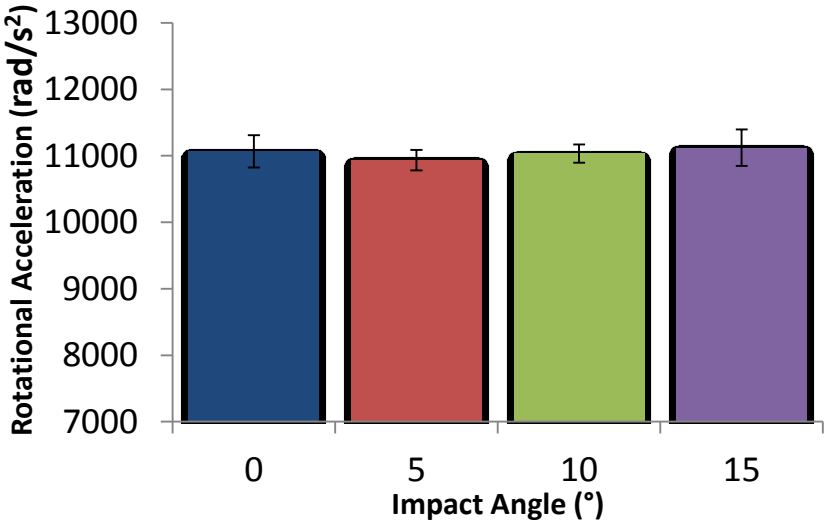

Figure 14: Peak resultant rotational accelerations (rad/s^2) for 0°, 5°, 10° and 15° impact angles at the side location with ± 1 standard deviation indicated in bars

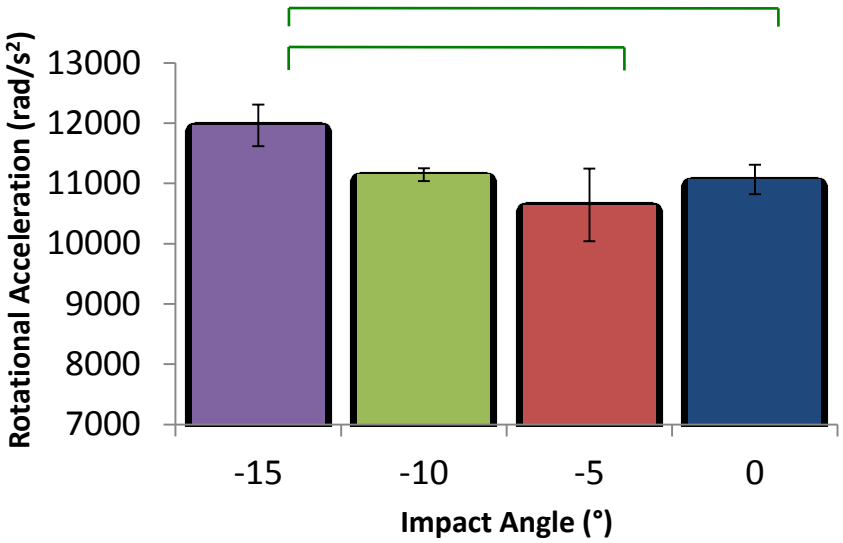

Figure 15: Peak resultant rotational accelerations (rad/s^2) for 0°, -5°, -10° and -15° impact angles at the side location with ± 1 standard deviation indicated in bars. Green bracket indicates significant comparisons

4.3 Maximum Principal Strain

For maximum principal strain, a significant main effect for impact angle was found at the front location [$F(3, 8) = 12.13$, $p = 0.002$) where the 15° condition (0.610) had significantly higher magnitudes of maximum principal strain than the 0° (0.515) and 5° conditions (0.496) at $p < 0.05$ for both comparisons (Figure 16).

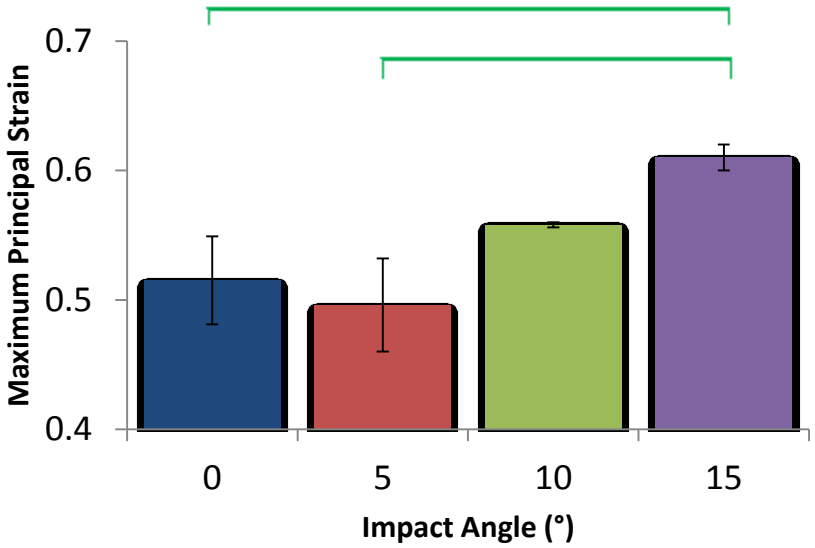

Figure 16: Peak maximum principal strain for 0°, 5°, 10° and 15° impact angles at the front location with ± 1 standard deviation indicated in bars. Green brackets indicate significant relationships

A significant main effect was found for impact angle at the side location [$F(6, 14) = 0.004$, $p < 0.001$]. For the positive angles (Figure 17), the only difference for maximum principal strain magnitudes were between the 10° condition (0.527) and the 15° condition (0.568) at $p = 0.024$. For the negative impact angles (Figure 18), the -10° (0.602) and -15° (0.634) impact conditions produced higher magnitudes of maximum principal strains than the 0° (0.557) and -5° (0.561) conditions ($p \leq 0.026$ for all comparisons). Additionally, the -10° and -15° conditions were not significantly different as observed for the positive angles ($p=0.106$).

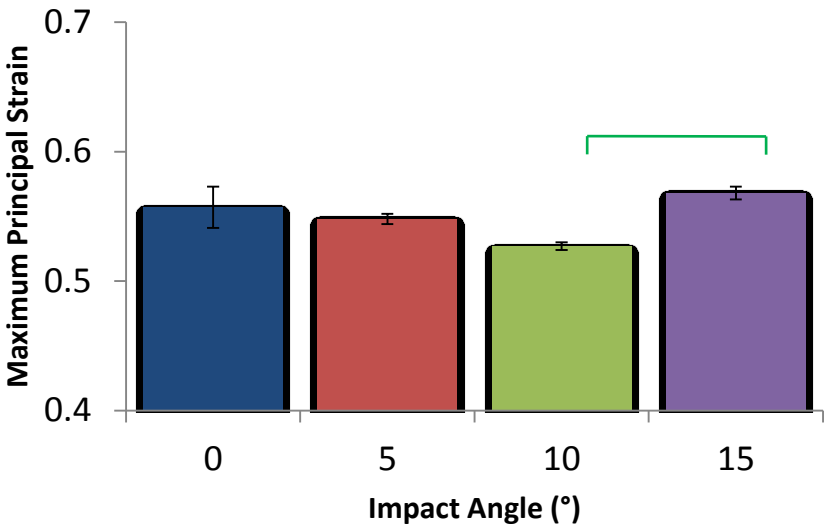

Figure 17: Peak maximum principal strain for 0°, 5°, 10° and 15° impact angles at the side location with ± 1 standard deviation indicated in bars. A green bracket indicates a significant relationship

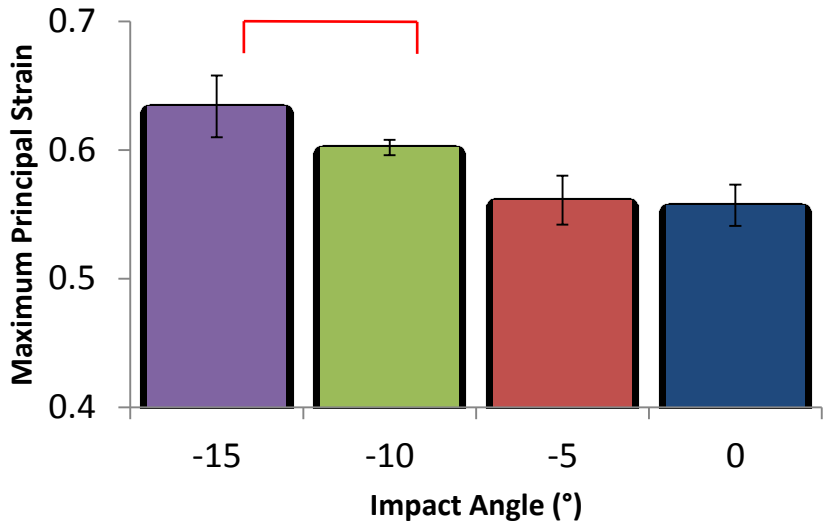

Figure 18: Peak maximum principal strain for 0°, -5°, -10° and -15° impact angles at the side location with ± 1 standard deviation indicated in bars. A red bracket indicates no significant relationship between angles

4.4 Von Mises Stress

For von Mises stress, a significant main effect was only found for impact angle at the front location [$F(3, 8) = 12.21$, $p = 0.002$]. The 15° condition (18.77 kPa) produced higher magnitudes of von Mises stress than the 0, 5 and 10° conditions (15.89, 15.23 and 16.62 kPa respectively) at $p < 0.05$. The results for von Mises stress at the front are shown in Figure

19. The results for von Mises stress at the side for both positive and negative angles are illustrated in Figure 20 and Figure 21.

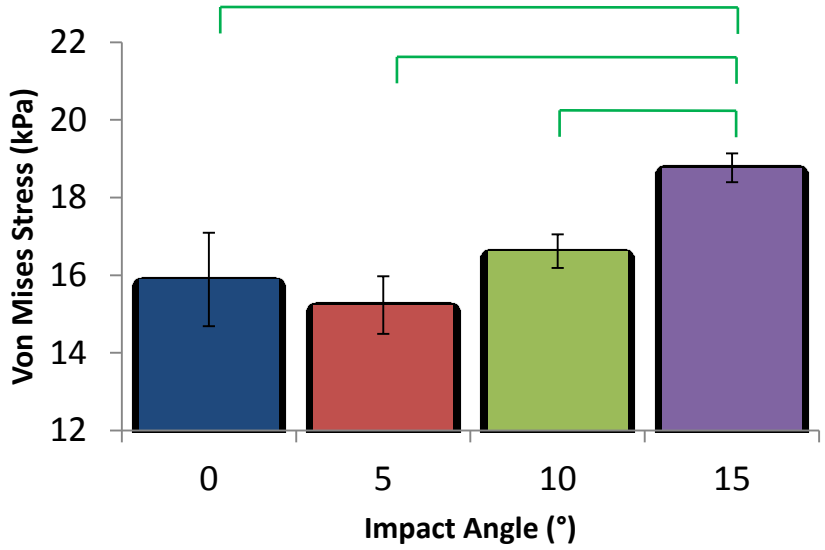

Figure 19: Peak von Mises stress (kPa) for 0°, 5°, 10° and 15° impact angles at the front location with ± 1 standard deviation indicated in bars. Green brackets indicate significant relationships

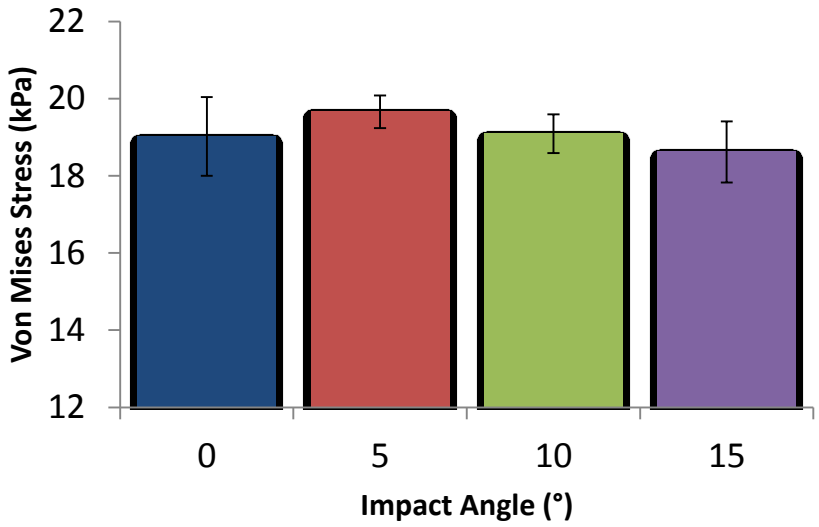

Figure 20: Peak von Mises stress (kPa) for 0°, 5°, 10° and 15° impact angles at the side location with ± 1 standard deviation indicated in bars

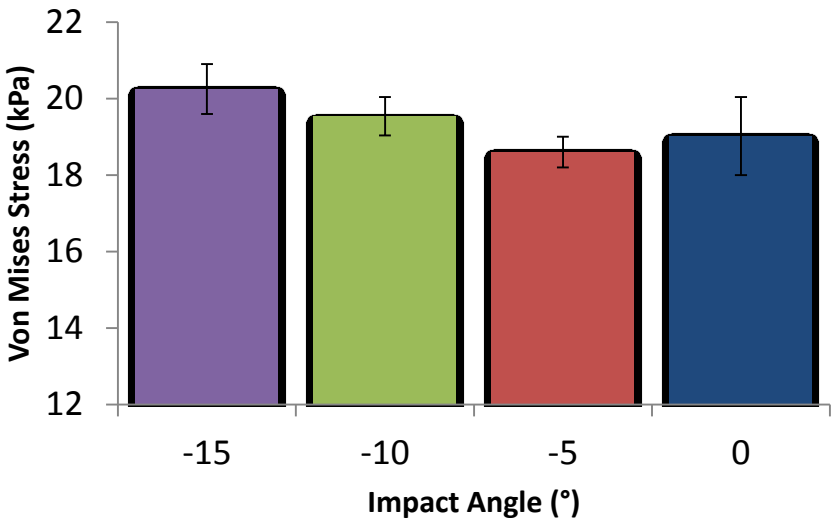

Figure 21: Peak von Mises stress (kPa) for 0°, -5°, -10° and -15° impact angles at the side location with ± 1 standard deviation indicated in bars

A summary of the results are presented in Table 5 where at least a 10° angle was necessary to create a statistical difference for rotational acceleration at the front location and maximum principal strain at the side location amongst the negative angles. At least a 15° angle was necessary to create statistically different effects for von Mises stress at the front, maximum principal strain at the front and the positive angles at the side and linear and rotational accelerations at the negative angles for the side.

Table 5: Summary of the influence of impact angle on the dynamic response of a Hybrid III headform and brain tissue deformation

	Front	Side (+)	Side (-)
Linear Acceleration (g)			15°
Rotational Acceleration (rad/s^2)	10°		15°
Maximum Prinicpal Strain	15°	15°	10°
Von Mises Stress	15°		

5. Discussion

When studying head impact conditions producing injury, it would be appropriate to understand how different factors affect the response of the head and brain to impact. Impact angle has been identified as a contributing parameter that influences headform dynamic response (Walsh, Rousseau et al., 2011); however the isolation of this variable and its affect alone is not well understood. The objective of this study was to investigate the influence of impact angle on the dynamic response of a Hybrid III headform by measuring peak resultant linear and rotational acceleration and estimating peak maximum principal strain and von Mises stress with a finite element model of the brain.

5.1 Headform Dynamic Response

When examining headform dynamic response using acceleration, the effect of impact angle on the results is asymmetrical about the location of the headform as well as the dependent variable. For linear acceleration, angle only had an effect for the negative angles at the side. When using rotational acceleration, angle had an effect at both the front and side location but only for the negative angles at the side. These asymmetries in the results may be reflective of the sensitivity of the front and side locations of the headform to a change in impact angle. These differences in head acceleration seen across impact angle can be attributed to physical characteristics of the head and neckform that would affect its motion at impact, such as the geometry of the headform, the non-uniform distribution of mass as well as characteristics of the neckform.

The different geometries at the front and side locations of the Hybrid III headform could have contributed to the differences seen across impact angle. In a combination with the non-uniform distribution of mass of the headform, this would have resulted in distinct

headform motions when impact angle was varied at the two different locations as well as the direction of angle at the side location.

Willinger, Baumgartner et al. (2001) recorded moments of inertia for the Hybrid III headform. They reported $1.590 \cdot 10^{-2}$ kg· m^2 in the x axis, $2.400 \cdot 10^{-2}$ kg· m^2 in the y axis and $2.200 \cdot 10^{-2}$ kg· m^2 in the z axis, where positive x, y and z axes are oriented to the front, leftwards and upwards (Willinger, Baumgartner et al., 2001). The higher moment of inertia about the y axis ($2.400 \cdot 10^{-2}$ kg· m^2) causing anterior-posterior rotation could help to explain why lower magnitudes of rotational acceleration are found for front impacts as compared to the side impacts ($1.590 \cdot 10^{-2}$ kg· m^2 in the x axis). In this current study, off-axes moments of inertia that deviate from the x, y and z axes are currently unknown and it is difficult to state the degree to which moment of inertia affects the motion of the headform when impact angle is changed. However, since the moments of inertia of the Hybrid III headform is asymmetrical about the x, y and z axes and is a reflection of the non-uniform distribution of mass, it is likely that this mass distribution would also affect headform acceleration when impacted off axis as a result of a change in angle.

An additional factor that may influence the results is the vinyl rubber skin covering the steel headform. Although the thickness of the skin at the impact locations are similar (1.1 and 1.2 cm respectively for the front and side), the interaction of the skin and the impactor striker as well as the skin and the steel headform are unknown which could also influence the dynamic response of the headform.

The Hybrid III neckform could also have had an effect on the results. The neckform was composed of four butyl rubber disks interlocked between five aluminum plates with slits on the anterior portion of the neckform to allow for different responses in neck flexion

than extension (Ashrafiuon, Colbert et al., 1996). Since the neckform has an asymmetrical response to motion, this effect may contribute to the differences in headform acceleration across impact angles.

Previous work by Foreman (2010) supports this notion of neck asymmetry. The author performed neckform quasi-static tests at 100mm/min to measure directional neck compliance during bending (Foreman, 2010). It was found that neckform compliance in extension (frontal loading) was much higher than compliance in lateral bending (side loading) where increased magnitudes of headform acceleration were found for side impacts as compared to front impacts (Foreman, 2010).

In a separate study by Rousseau, Hoshizaki et al. (2010), these researchers compared separate neckforms with three different levels of compliance. In this study, the authors found that decreased neckform compliance produced lower values of rotational acceleration whereas a more compliant or softer neckform produced higher values of rotational acceleration (Rousseau, Hoshizaki et al., 2010). In this research, the authors only compared neckform compliance using frontal impacts directed at a Hybrid III headform (Rousseau et al., 2010) and it is possible that the anisotropic characteristics of the neckform may produce difference responses if impacted in other directions.

Walsh, Rousseau et al. (2011), studied the effect of impact location and angle using a large impactor striker (Figure 1) on the response of a Hybrid III head and neckform. These authors identified specific impact conditions that are composed of a combination of location and angle that created high linear accelerations and low rotational accelerations when the impact was primarily directed through the center of gravity of the headform (near centric), and those that created low linear accelerations and high rotational accelerations when the

impact was directed off center (non-centric) creating more of a rotation. When impact angle was varied, this created a non-centric condition and resulted in larger changes in magnitudes of acceleration (Walsh, Rousseau et al., 2011) as compared to the results observed in this current study when angle was varied.

These differences observed in the results between the two studies are due to the impactor striker that was used. Since Walsh, Rousseau et al. (2011) used a larger diameter striker, this caused the side of the striker to impact a different location on the headform which created a distinct non-centric condition. When compared to the impact conditions in this study, when angle was increased (also resulting in a non-centric impact), the line of impact is much closer to the centre of gravity of the headform as compared to those that are defined in the (Walsh, Rousseau et al., 2011), this would explain why dissimilar results were observed between the two studies.

Since smaller changes in accelerations were observed between impact angle conditions in this study as compared to the results in Walsh, Rousseau et al. (2011), it is much more likely that higher severity impacts are a function of how non-centric the line of impact is as compared to a change in impact angle alone.

5.2 Brain Tissue Deformation

Similar relationships can be found for impact angle and brain tissue deformation. This is expected since the maximum principal strain and von Mises stress are derived from the linear and rotational acceleration-time histories.

At the front impact location, the 15° angle produced higher magnitudes of maximal principal strain and von Mises stress than the lower impact angles of 0 and 5° which are

similar to the results for headform acceleration. When examining the side location using these variables, a different relationship was found where impact angle only influenced magnitudes of maximum principal strain and not von Mises stress. For the positive impact angles, a 15° angle produced higher magnitudes of maximum principal strain than the 10° condition. Meanwhile for the negative impact angles, the greater the angles (-10 and -15°) produced higher magnitudes of MPS than the 0 and -5° conditions.

In a study evaluating helmets using a centric and non-centric impact protocol, Post, Oeur et al. (2011) correlated headform linear and rotational accelerations with brain tissue stress and strain and found that rotational acceleration was moderately correlated with maximum principal strain ($r = 0.64$) and von Mises stress ($r = 0.67$), meanwhile only a negative low correlation was found for linear acceleration and maximum principal strain ($r = -0.24$) (Post, Oeur et al., 2011). Similarly, Forero Rueda, Cui et al. (2011) found that maximum principal strain and von Mises stress had better relationships with rotational acceleration ($R^2 = 0.70$ and 0.72, respectively) than linear acceleration ($R^2 = 0.47$ and 0.52, respectively). The larger magnitudes of maximum principal strain and von Mises stress found for the larger impact angles could be explained by the increased rotational acceleration at these conditions when compared to the 0° condition.

Characteristics of the acceleration-time curves of each component of linear and rotational acceleration could also help to explain the differences in magnitudes observed in brain tissue deformation variables. Since the linear and rotational accelerations are used as input into the finite element model of the brain, the resulting brain tissue deformations measured using maximum principal strain and von Mises stress would be influenced by these headform dynamic response measures. It has been proposed that the constitutive

material properties and laws governing the different types of brain tissue in the finite element model used for analysis would influence the magnitudes of brain tissue deformation (Schreiber, Bain et al., 1997, Post, Hoshizaki et al., 2012). Both linear and rotational accelerations are composed of x, y and z axes of acceleration and minute changes in one of these components could help to explain why varying magnitudes of brain tissue deformation exists within the data.

Examples of the linear and rotational acceleration-time histories are presented in Appendix A, where Figure 22 is the acceleration-time curves for the front location and Figure 23 are the curves for the side location. When examining the linear acceleration-time curves for the front impact location, the resultant curve (black line) and the acceleration about the x axis (red line) are similar in shape and magnitude between the front 0° and front 15° condition. When examining the accelerations about the y and z axes, the front 15° condition has slightly larger amplitudes of accelerations for both axes of acceleration than the front 0° condition. In the case for rotational acceleration, the resultant curve and the y axis acceleration are similar for both impact angles, meanwhile the x and z accelerations have slightly greater amplitudes for the 15° condition.

When examining the linear acceleration-time curves at the side impact location, it can be seen the resultant curve and the y axis acceleration across all angles are similar, with the y axis acceleration closely following that of the resultant. When comparing the +15 and -15° conditions to the 0° condition, both the x and z acceleration-time curves are slightly larger in magnitude for linear acceleration. For the rotational acceleration-time curves, the y and z axes accelerations are slightly greater in amplitude for the +15 and -15° conditions

when compared to the 0° condition, meanwhile the peak resultant acceleration-time curve remains similar across all three conditions.

A separate study by Walsh & Hoshizaki (2010) also found that variations in inbound vector angle altered component accelerations, that is the x, y and z component accelerations that make up the resultant acceleration. They concluded peak resultant acceleration values may not fully describe the headform dynamic response (Walsh & Hoshizaki, 2010). It is important to note that the authors used a flat impacting anvil for this research in order to study the sensitivity of angle variation; however using a flat anvil to study impact angle becomes problematic as interactions between the anvil and the headform would make it difficult to isolate impact angle as a variable. Therefore, peak resultant linear and rotational accelerations may not fully capture the effect of impact angle and that brain tissue deformation may be a better measure since it incorporates all three axes of headform linear and rotational acceleration.

In a study by Post, Hoshizaki et al. (2012), characteristics of the acceleration-time curve in each of the x, y and z axis was shown to influence the magnitudes of brain tissue deformation. Some of the curve characteristics that were found to influence brain tissue deformation were magnitude of the peak as well as the time-to peak. It was found that acceleration-time curves with high peaks as well as a longer time-to-peak produced higher magnitudes of maximum principal strain and von Mises stress than those that had lower peaks and a shorter time-to-peaks (Post, Hoshizaki et al., 2012).

5.3 Significance of Study

Although significant magnitudes of headform acceleration and brain tissue deformation were found in the results, these differences may not be a meaningful difference when evaluated in the context brain injury thresholds. For example, the side -15° condition (11 964 rad/s^2) produced significantly higher magnitudes of acceleration than the side 0° impact condition (11 067 rad/s^2); however the absolute difference between these levels of acceleration is only approximately 900 rad/s^2 which is only an 8% increase in acceleration. An increase of 8% in rotational acceleration may not be a large enough difference to have any implications regarding the role of impact angle in contributing to injurious levels of acceleration.

Zhang, Yang & King (2004) proposed a threshold for concussive injury based on head injury reconstructions of American football player collisions. A summary of their proposed thresholds for a 25%, 50% and 80% probability of concussion is presented below (). When examining the results of this study in light of this threshold, it is evident that the magnitudes of headform acceleration as well as brain tissue deformation are well over the 80% probability for concussion.

Table 6. Summary of the proposed concussive injury threshold by Zhang, Yang & King (2004)

	Probability of Concussion		
Variable	25%	50%	80%
Linear Acceleration (g)	66	82	106
Rotational Acceleration (rad/s^2)	4600	5900	7900
Strain	0.14	0.19	0.24
Shear Stress (kPa)	6	7.8	10

Since the levels of acceleration and brain tissue deformation in this study are likely to cause concussion based on the threshold proposed by Zhang, Yang et al. (2004b), it is difficult to identify the implications of impact angle on producing brain injury. The conditions for head impact in this study create headform dynamic responses that are too high to allow for an appropriate comparison. It may be interesting to perform the head impacts conducted in this study on a helmeted headform to decrease the level of headform dynamic response and brain tissue deformations to a range that is within proposed thresholds for concussive brain injury. The goal of a helmet is to mitigate the energy from an impact to the head (Hoshizaki and Brien, 2004). Since the relationships found in this study for impact angle would remain the same, the use of a helmet would lower the magnitudes of headform acceleration and subsequently brain tissue deformation to a range for concussive injury. This may provide interesting information regarding the role of impact angle in the production of injurious levels of acceleration and brain tissue deformation.

The results observed in this study are specific to the test rig and materials used in the study. For example, the Hybrid III head and neckform have been reported to influence the results. Also, the results in this study are specific to the finite element model used for analysis as the brain tissue deformation variables estimated from the dynamic response of the headform are characteristic of the constitutive tissue properties and material laws governed by the finite element model. In order to fully understand impact angle on the headform dynamic response, future work could entail studying the effect of impact angle at different locations on the headform to better understand the effect of the neck on the headform dynamic response as well as brain tissue deformation. Specifically, it may be interesting to see how the interaction between the head and neckform at a rear impact (least

compliant neckform direction) influence the dynamic response and brain tissue deformation at different impact angles. In order to appropriately isolate impact angle as a variable in this study, much effort was placed on ensuring that the apex of the striker impacted the same impact location across all conditions of angle. This limited the number of impact angles possible because the conditions were affected by the geometry of the headform and the striker.

Due to the absolute differences in accelerations and brain tissue deformation across each of the impact conditions, the results also suggest that impact angle alone may be less influential in creating injurious head responses to impact than other parameters that describe a head injury event. For example, impact location and velocity may be more important parameters that affect the response of the head to an impact as past animal research has identified these two parameters to affect the type and severity of brain injury observed (Unterharnscheidt, 1972, Gennarelli, Thibault et al., 1982). However, as mentioned previously, impact angle may contribute to producing injurious accelerations in a combination with impact location by creating centric and non-centric impact conditions (Walsh, Rousseau et al., 2011). It is also more likely that higher severity impacts are a function of how non-centric the line of impact is.

The study provides some insight into characteristics of the impact condition where geometry of the impacting objects seems to be an important parameter to consider in head impact analyses as geometry of the striker limits the number of possible impact angles directed at the headform. Also, the results from this study suggest that an impact angle variation of 15° would influence the results of a head impact analysis. This information can help to inform researchers about the sensitivity of impact angle in head injury reconstruction

where selecting appropriate impact angles would improve the reliability of the reconstruction.

6. Conclusion

6.1 Summary

Head impact angle is one of the variables that can be used to describe a head injury event. This study investigated the influence of impact angle on the dynamic response of a Hybrid III headform and brain tissue deformation. Peak kinematic measures alone may not be subtle enough to measure certain parameters such as impact angle where this study supports the use of finite element analysis when evaluating head impact variables.

The results suggest that an impact angle variation of 15° will create significantly different peak resultant linear and rotational accelerations as well as brain tissue deformations at the front and side impact locations depending on the measures used for comparison. These results are specific to the test conditions used in this study such as the Hybrid III headform, pointed impactor striker as well as the 5.5 m/s impact velocity. Due to the absolute differences in the magnitudes in each of the dependent variables, these differences may not be meaningful differences because impact angle produces such small changes in acceleration or stress and strain. As a result, impact angle alone may not be as important as a variable when studying head impact biomechanics and may produce more injurious conditions when combined with impact location in creating non-centric impact conditions.

7. References

Alves, W., S. N. Macciocchi and J. T. Barth (1993). "Postconcussive symptoms after uncomplicated mild head injury." *The Journal of Head Trauma Rehabilitation* **8**(3): 48-59.

Ashrafiuon, H., R. Colbert, L. Obergefell and I. Kaleps (1996). "Modeling of a deformable manikin neck for multibody dynamic simulation." *Mathematical and Computer Modelling* **24**(2): 45-56.

Association, C. S. (2009). Ice Hockey Helmets. *Z262.1-09*. Mississauga, Ontario, Canada.

Bailes, J. E. (2009). "Sports-related concussion: what do we know in 2009-a neurosurgeon's perspective." *J Int Neuropsychol Soc* **15**(4): 509-511.

Blinman, T. A., E. Houseknecht, C. Snyder, D. J. Wiebe and M. L. Nance (2009). "Postconcussive symptoms in hospitalized pediatric patients after mild traumatic brain injury." *J Pediatr Surg* **44**(6): 1223-1228.

Cantu, R. C. (1992). "Cerebral Concussion in Sport: Management and Prevention 1." *Sports Medicine* **14**(1): 64-74.

Delaney, J. S., V. J. Lacroix, S. Leclerc and K. M. Johnston (2002). "Concussions Among University Football and Soccer Players." *Clinical Journal of Sport Medicine* **12**(6): 331-338.

Dimasi, F. P., R. H. Eppinger and F. A. Bandak (1995). Computational analysis of head impact response under car crash loadings. *SAE PUBLICATION P-299. PROCEEDINGS OF THE 39TH STAPP CAR CRASH CONFERENCE, NOVEMBER 8-10, 1995, SAN DIEGO, CALIFORNIA, USA (SAE TECHNICAL PAPER 952718)*.

Dischinger, P. C., G. E. Ryb, J. A. Kufera and K. M. Auman (2009). "Early predictors of postconcussive syndrome in a population of trauma patients with mild traumatic brain injury." *J Trauma* **66**(2): 289-296; discussion 296-287.

Fijalkowski, R. J., B. D. Stemper, F. A. Pintar, N. Yoganandan, M. J. Crowe and T. A. Gennarelli (2007). "New rat model for diffuse brain injury using coronal plane angular acceleration." *J Neurotrauma* **24**(8): 1387-1398.

Foreman, S. G. (2010). *The Dynamic Impact Response of a Hybrid III Head- and Neckform under Four Neck Orientations and Three Impact Locations*. M.Sc. MR74136, University of Ottawa (Canada).

Forero Rueda, M. A., L. Cui and M. D. Gilchrist (2011). "Finite element modelling of equestrian helmet impacts exposes the need to address rotational kinematics in future helmet designs." *Comput Methods Biomech Biomed Engin* **14**(12): 1021-1031.

Foundation, S. M. (2010). 2010 Standard for Protective Headgear. North Highlands, California.

Frechede, B. and A. McIntosh (2007). Use of MADYMO's human facet model to evaluate the risk of head injury in impact. *Proceedings of the 21st ESV , conference paper No. 07-0300*, Lyon, France, NHTSA.

Gennarelli, T., A. Ommaya and L. Thibault (1971). Comparison of translational and rotational head motions in experimental cerebral concussion. *Proc. 15th Stapp Car Crash Conference*.

Gennarelli, T., L. E. Thibault, G. Tomei, R. Wiser, D. Graham and J. Adams (1987). "Directional Dependence of Axonal Brain Injury due to Centroidal and Non-Centroidal Acceleration." *SAE Technical Paper 872197*.

Gennarelli, T. A. (1994). "Animate models of human head injury." *Journal of Neurotrauma* **11**(4): 357-368.

Gennarelli, T. A., L. E. Thibault, J. H. Adams, D. I. Graham, C. J. Thompson and R. P. Marcincin (1982). "Diffuse axonal injury and traumatic coma in the primate." *Ann Neurol* **12**(6): 564-574.

Gerberich, S. G., J. D. Priest, J. R. Boen, C. P. Straub and R. E. Maxwell (1983). "Concussion incidences and severity in secondary school varsity football players." *Am J Public Health* **73**(12): 1370-1375.

Gessel, L. M., S. K. Fields, C. L. Collins, R. W. Dick and R. D. Comstock (2007). "Concussions among United States high school and collegiate athletes." *J Athl Train* **42**(4): 495-503.

Gilchrist, M. D. and D. O'Donoghue (2000). "Simulation of the development of frontal head impact injury." *Computational Mechanics* **26**(3): 229-235.

Gordon, K. E., J. M. Dooley and E. P. Wood (2006). "Descriptive epidemiology of concussion." *Pediatr Neurol* **34**(5): 376-378.

Groat, R. A., W. F. Windle and H. W. Magoun (1945). "Functional and Structural Changes in the Monkey's Brain During and After Concussion*." *Journal of Neurosurgery* **2**(1): 26-35.

Gross, A. G. (1958). "A new theory on the dynamics of brain concussion and brain injury." *J Neurosurg* **15**(5): 548-561.

Gurdjian, E. S. (1972). "Recent advances in the study of the mechanism of impact injury of the head--a summary." *Clin Neurosurg* **19**: 1-42.

Gurdjian, E. S., V. R. Hodgson, L. M. Thomas and L. M. Patrick (1968). "Significance of relative movements of scalp, skull, and intracranial contents during impact injury of the head." *J Neurosurg* **29**(1): 70-72.

Gurdjian, E. S., H. R. Lissner, J. E. Webster, F. R. Latimer and B. F. Haddad (1954). "Studies on experimental concussion: relation of physiologic effect to time duration of intracranial pressure increase at impact." *Neurology* **4**(9): 674-681.

Gurdjian, E. S., J. E. Webster and H. R. Lissner (1955). "Observations on the mechanism of brain concussion, contusion, and laceration." *Surg Gynecol Obstet* **101**(6): 680-690.

Hardy, W. N., C. D. Foster, M. J. Mason, K. H. Yang, A. I. King and S. Tashman (2001). "Investigation of head injury mechanisms using neutral density technology and high-speed biplanar X-ray." *Stapp Car Crash Journal* **45**(SAE P-375, 2001-22-0016).

Hardy, W. N., M. J. Mason, C. D. Foster, C. S. Shah, J. M. Kopacz, K. H. Yang, A. I. King, J. Bishop, M. Bey, W. Anderst and S. Tashman (2007). "A study of the response of the human cadaver head to impact." *Stapp Car Crash J* **51**: 17-80.

Hodgson, V., L. Thomas and T. Khalil (1983). The role of impact location in reversible cerebral concussion. *Twenty-Seventh Stapp Car Crash Conference Proceedings (P-134) with International Research Committee on Biokinetics of Impacts (IRCOBI), San Diego, California, October 17-19, 1983.*

Holbourn, A. H. S. (1943). "MECHANICS OF HEAD INJURIES." *The Lancet* **242**(6267): 438-441.

Horgan, T. J. (2005). *A finite element model of the human head for use in the study of pedestrian accidents*. Doctoral Dissertation, University College Dublin.

Horgan, T. J. and M. D. Gilchrist (2003). "The creation of three-dimensional finite element models for simulating head impact biomechanics." *International Journal of Crashworthiness* **8**(4): 353-366.

Horgan, T. J. and M. D. Gilchrist (2004). "Influence of FE model variability in predicting brain motion and intracranial pressure changes in head impact simulations." *International Journal of Crashworthiness* **9**(4): 401-418.

Hoshizaki, T. B. and S. E. Brien (2004). "The science and design of head protection in sport." *Neurosurgery* **55**(4): 956-966; discussion 966-957.

Kelly, J. P., J. S. Nichols, C. M. Filley, K. O. Lillehei, D. Rubinstein and B. K. Kleinschmidt-DeMasters (1991). "Concussion in sports. Guidelines for the prevention of catastrophic outcome." *JAMA* **266**(20): 2867-2869.

Kelly, J. P. and J. H. Rosenberg (1997). "Diagnosis and management of concussion in sports." *Neurology* **48**(3): 575-580.

Khan, K. M. (2009). "Improving health & performance: nutritional supplements, science of pacing, and the concussion tool (SCAT2)." *British Journal of Sports Medicine* **43**(10): 727-727.

King, A. I., K. H. Yang, L. Zhang, W. Hardy and D. C. Viano (2003). Is head injury caused by linear or angular acceleration. *IRCOBI conference*.

Kleiven, S. (2003). "Influence of impact direction on the human head in prediction of subdural hematoma." *J Neurotrauma* **20**(4): 365-379.

Kleiven, S. (2007). "Predictors for traumatic brain injuries evaluated through accident reconstructions." *Stapp Car Crash J* **51**: 81-114.

Le Bihan, D., J. F. Mangin, C. Poupon, C. A. Clark, S. Pappata, N. Molko and H. Chabriat (2001). "Diffusion tensor imaging: concepts and applications." *J Magn Reson Imaging* **13**(4): 534-546.

McClincy, M. P., M. R. Lovell, J. Pardini, M. W. Collins and M. K. Spore (2006). "Recovery from sports concussion in high school and collegiate athletes." *Brain Inj* **20**(1): 33-39.

McCrea, M., K. M. Guskiewicz, S. W. Marshall, W. Barr, C. Randolph, R. C. Cantu, J. A. Onate, J. Yang and J. P. Kelly (2003). "Acute effects and recovery time following concussion in collegiate football players: the NCAA Concussion Study." *JAMA* **290**(19): 2556-2563.

McCrory, P., W. Meeuwisse, K. Johnston, J. Dvorak, M. Aubry, M. Molloy and R. Cantu (2009). "Consensus statement on concussion in sport - the Third International Conference on Concussion in Sport held in Zurich, November 2008." *Phys Sportsmed* **37**(2): 141-159.

Meaney, D. F. and D. H. Smith (2011). "Biomechanics of Concussion." *Clinics in sports medicine* **30**(1): 19-31.

Nahum, A. M., R. Smith and C. C. Ward (1977). Intracranial pressure dynamics during head impact. *21st Stapp Car Crash Conference, SAE*.

Neurology, A. A. o. (1997). "Practice parameter: the management of concussion in sports (summary statement). Report of the Quality Standards Subcommittee." *Neurology* **48**(3): 581-585.

Newman, J. A., M. C. Beusenberg, E. Fournier, N. Shewchenko, C. Withnall, A. I. King, L. Zhang, J. McElhaney, L. E. Thibault and G. McGinnes (1999). A new biomechanical assessment of mild traumatic brain injury. Part 1: methodology. *Proceedings of the 1999 IRCOBI Conference on the Biomechanics of Impact*.

Newman, J. A., M. C. Beusenberg, N. Shewchenko, C. Withnall and E. Fournier (2005). "Verification of biomechanical methods employed in a comprehensive study of mild

traumatic brain injury and the effectiveness of American football helmets." *Journal of Biomechanics* **38**(7): 1469-1481.

Niogi, S. N., P. Mukherjee, J. Ghajar, C. Johnson, R. A. Kolster, R. Sarkar, H. Lee, M. Meeker, R. D. Zimmerman, G. T. Manley and B. D. McCandliss (2008). "Extent of microstructural white matter injury in postconcussive syndrome correlates with impaired cognitive reaction time: a 3T diffusion tensor imaging study of mild traumatic brain injury." *AJNR American journal of neuroradiology* **29**(5): 967-973.

O'Riordain, K., P. M. Thomas, J. P. Phillips and M. D. Gilchrist (2003). "Reconstruction of real world head injury accidents resulting from falls using multibody dynamics." *Clinical Biomechanics* **18**(7): 590-600.

Omalu, B. I., S. T. DeKosky, R. L. Minster, M. I. Kamboh, R. L. Hamilton and C. H. Wecht (2005). "Chronic Traumatic Encephalopathy in a National Football League Player." *Neurosurgery* **57**(1): 128-134 110.1227/1201.NEU.0000163407.0000192769.ED.

Padgaonkar, A. J., K. W. Krieger and A. I. King (1975). "Measurement of Angular Acceleration of a Rigid Body Using Linear Accelerometers." *Journal of Applied Mechanics* **42**(3): 552-556.

Pellman, E. J., D. C. Viano, A. M. Tucker, I. R. Casson and N. F. L. Committee on Mild Traumatic Brain Injury (2003a). "Concussion in professional football: location and direction of helmet impacts-Part 2." *Neurosurgery* **53**(6): 1328-1340; discussion 1340-1321.

Pellman, E. J., D. C. Viano, A. M. Tucker, I. R. Casson and J. F. Waeckerle (2003b). "Concussion in Professional Football: Reconstruction of Game Impacts and Injuries." *Neurosurgery* **53**(4): 799-814 710.1227/1201.NEU.0000083559.0000068424.0000083553F.

Pellman, E. J., D. C. Viano, C. Withnall, N. Shewchenko, C. A. Bir and P. D. Halstead (2006). "Concussion in professional football: helmet testing to assess impact performance--part 11." *Neurosurgery* **58**(1): 78-96; discussion 78-96.

Post, A., B. Hoshizaki and M. D. Gilchrist (2012). "Finite element analysis of the effect of loading curve shape on brain injury predictors." *J Biomech* **45**(4): 679-683.

Post, A., A. Oeur, B. Hoshizaki and M. D. Gilchrist (2011). "Examination of the relationship between peak linear and angular accelerations to brain deformation metrics in hockey helmet impacts." *Comput Methods Biomech Biomed Engin*.

Rousseau, P. and T. B. Hoshizaki (2009). "The influence of deflection and neck compliance on the impact dynamics of a Hybrid III headform." *Proceedings of the Institution of Mechanical Engineers, Part P: Journal of Sports Engineering and Technology* **223**(3): 89-97.

Rousseau, P., T. B. Hoshizaki, M. D. Gilchrist and A. Post (2010). "Estimating the influence of neckform compliance on brain tissue strain during a Helmeted impact." *Stapp Car Crash J* **54**: 37-48.

Schreiber, D. I., A. C. Bain and D. F. Meaney (1997). In vivo thresholds for mechanical injury to the blood brain barrier. *41st Stapp Car Crash Conference, SAE paper No. 973335*.

Shaw, N. A. (2002). "The neurophysiology of concussion." *Progress in Neurobiology* **67**(4): 281-344.

Smith, D., K. Uryu, K. Saatman, J. Trojanowski and T. McIntosh (2003). "Protein accumulation in traumatic brain injury." *NeuroMolecular Medicine* **4**(1): 59-72.

Trosseille, X., C. Tarriere, F. Lavaste, F. Guillon and A. Domont (1992). Development of a FEM of the human head according to a specific test protocol. *36th Stapp Car Crash Conference, SAE*.

Ueno, K., J. W. Melvin, L. Li and J. W. Lighthall (1995). "Development of tissue level brain injury criteria by finite element analysis." *J Neurotrauma* **12**(4): 695-706.

Unterharnscheidt, F. J. (1972). "Translational versus rotational acceleration: animal experiments with measured input." *Scand J Rehabil Med* **4**(1): 24-26.

van Donkelaar, P., J. Langan, E. Rodriguez, A. Drew, C. Halterman, L. R. Osternig and L.-S. Chou (2005). "Attentional deficits in concussion." *Brain Injury* **19**(12): 1031-1039.

Viano, D. C., I. R. Casson, E. J. Pellman, L. Zhang, A. I. King and K. H. Yang (2005). "Concussion in professional football: brain responses by finite element analysis: part 9." *Neurosurgery* **57**(5): 891-916; discussion 891-916.

Walsh, E., P. Rousseau and T. Hoshizaki (2011). "The influence of impact location and angle on the dynamic impact response of a Hybrid III headform." *Sports Engineering* **13**(3): 135-143.

Willinger, R. and D. Baumgartner (2003). "Human head tolerance limits to specific injury mechanisms." *International Journal of Crashworthiness* **8**(6): 605-617.

Willinger, R., D. Baumgartner, B. Chinn and E. Schuller (2001). "New dummy head prototype : development, validation and injury criteria." *International Journal of Crashworthiness* **6**(3): 281-294.

Willinger, R., L. Taleb and C. M. Kopp (1995). "Modal and temporal analysis of head mathematical models." *J Neurotrauma* **12**(4): 743-754.

Yoganandan, N. and F. A. Pintar (2004). "Biomechanics of temporo-parietal skull fracture." *Clinical Biomechanics* **19**(3): 225-239.

Yoganandan, N., F. A. Pintar, J. Zhang and J. L. Baisden (2009). "Physical properties of the human head: mass, center of gravity and moment of inertia." *Journal of Biomechanics* **42**(9): 1177-1192.

Zhang, L., K. Yang and A. King (2001a). "Biomechanics of neurotrauma." *Neurological Research* **23**(2-3): 144-156.

Zhang, L., K. H. Yang, R. Dwarampudi, K. Omori, T. Li, K. Chang, W. N. Hardy, T. B. Khalil and A. I. King (2001b). "Recent advances in brain injury research: a new human head model development and validation." *Stapp Car Crash J* **45**: 369-394.

Zhang, L., K. H. Yang and A. I. King (2001c). "Comparison of brain responses between frontal and lateral impacts by finite element modeling." *J Neurotrauma* **18**(1): 21-30.

Zhang, L., K. H. Yang and A. I. King (2004a). "A proposed injury threshold for mild traumatic brain injury." *J Biomech Eng* **126**(2): 226-236.

Zhang, L., K. H. Yang and A. I. King (2004b). "A Proposed Injury Threshold for Mild Traumatic Brain Injury." *Journal of Biomechanical Engineering* **126**(2): 226.

8. Appendix A

Head Impact Results for Thesis data and Pilot Data

Front 0

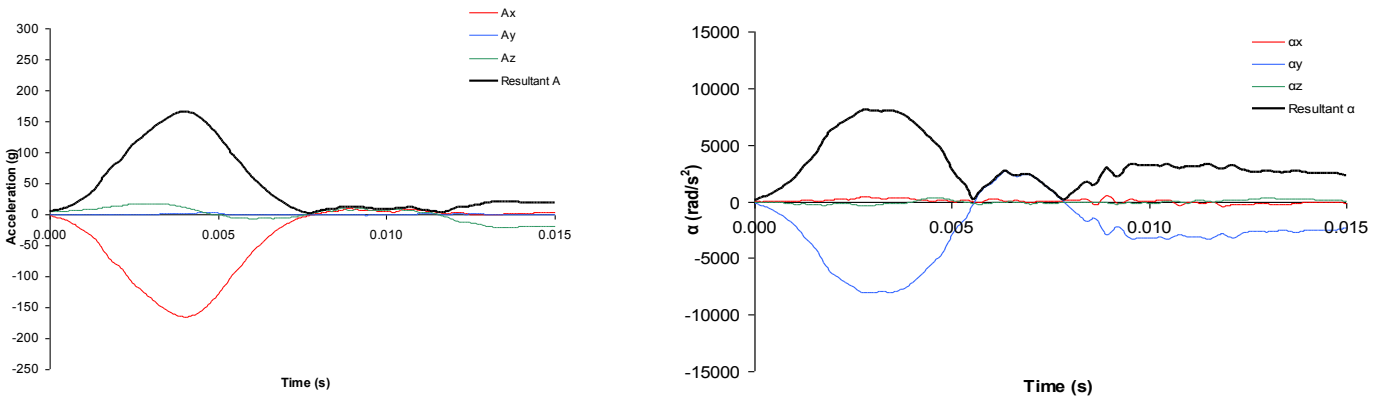

Front 15

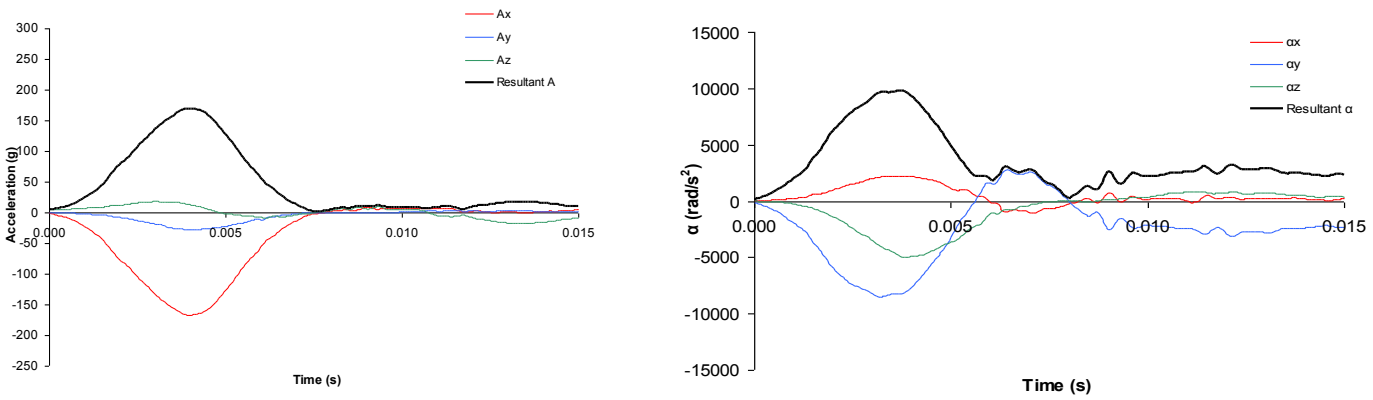

Figure 22: Linear (left) and rotational (right) acceleration-time curves for the front 0° (top) and front 15° (below)

Side

-15

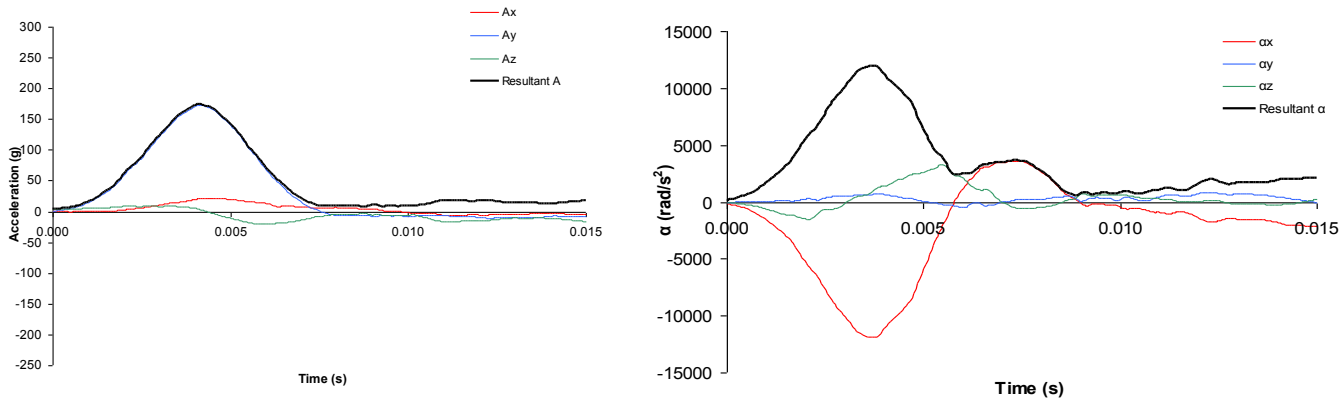

Side

0

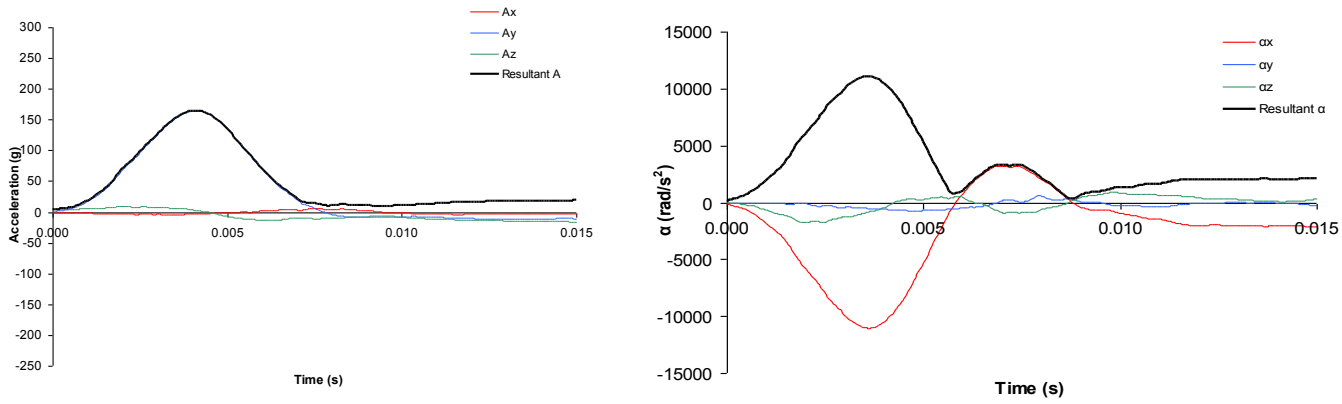

Side

+15

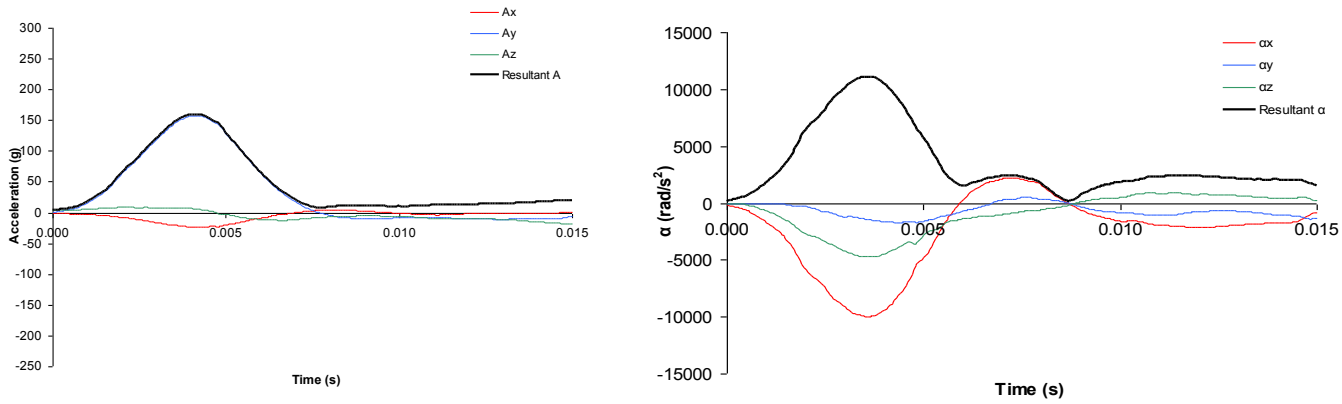

Figure 23: Linear (left) and rotational (right) acceleration-time curves for the side -15° (top), side 0° (middle) and side +15° (bottom) conditions

Table 7: Peak linear and rotational accelerations for the front and side impact locations for each trial

			Peak Resultant Acceleration	
Location	Angle (°)	Trial #	Linear (g)	Rotational (rad/s^2)
Front	0	1	164.7	7985
Front	0	2	166.4	8299
Front	0	3	165.6	7965
Front	5	1	165.8	8398
Front	5	2	161.5	8205
Front	5	3	159.4	8244
Front	10	1	159.3	8652
Front	10	2	167.9	8776
Front	10	3	169.7	8907
Front	15	1	171.7	10013
Front	15	2	169.1	9873
Front	15	3	168.7	9931
Side	0	1	156.5	10805
Side	0	2	168.9	11287
Side	0	3	168.7	11109
Side	5	1	165.3	11049
Side	5	2	160.6	10992
Side	5	3	161.1	10761
Side	10	1	162.1	10882
Side	10	2	160.7	11079
Side	10	3	161.4	11142
Side	15	1	161.5	11288
Side	15	2	158.5	10803
Side	15	3	159.4	11271
Side	-5	1	168	11315
Side	-5	2	162.8	10150
Side	-5	3	162.7	10462
Side	-10	1	173.8	11039
Side	-10	2	171.6	11147
Side	-10	3	169.6	11250
Side	-15	1	179.1	12363
Side	-15	2	172.1	11777
Side	-15	3	172.2	11752

Table 8: Peak maximum principal strain and von Mises stress for the front and side impact locations for each trial

			Brain Tissue Deformation	
Location	Angle (°)	Trial #	Maximum Principal Strain	Von Mises Stress (kPa)
Front	0	1	0.475	14.50
Front	0	2	0.535	16.51
Front	0	3	0.534	16.66
Front	5	1	0.508	15.82
Front	5	2	0.456	14.40
Front	5	3	0.524	15.49
Front	10	1	0.559	16.88
Front	10	2	0.556	16.12
Front	10	3	0.558	16.84
Front	15	1	0.602	18.55
Front	15	2	0.607	18.58
Front	15	3	0.622	19.20
Side	0	1	0.546	17.84
Side	0	2	0.575	19.60
Side	0	3	0.550	19.62
Side	5	1	0.551	20.13
Side	5	2	0.549	19.31
Side	5	3	0.543	19.55
Side	10	1	0.525	18.97
Side	10	2	0.525	19.65
Side	10	3	0.531	18.66
Side	15	1	0.570	19.53
Side	15	2	0.572	18.08
Side	15	3	0.563	18.27
Side	-5	1	0.582	18.71
Side	-5	2	0.548	18.16
Side	-5	3	0.552	18.94
Side	-10	1	0.608	20.08
Side	-10	2	0.600	19.43
Side	-10	3	0.597	19.10
Side	-15	1	0.661	20.99
Side	-15	2	0.617	19.74
Side	-15	3	0.624	20.04

Table 9: Peak resultant linear and rotational acceleration from a pilot study using the large impactor striker

			Peak Resultant Acceleration	
Location	Angle	Trial #	Linear (g)	Rotational (rad/s^2)
Side	0	1	98.1	9841
Side	0	2	97.9	10 042
Side	0	3	97.6	10 117
Side	30	1	47.9	5170
Side	30	2	46.6	5100
Side	30	3	47.5	5096